Monthly Notices of the ROYAL ASTRONOMICAL SOCIETY

MNRAS **520,** 1092–1110 (2023) https://doi.org/10.1093/mnras/stad013
Advance Access publication 2023 January 6

Photometric variable stars in the young open cluster NGC 6823

Sneh Lata,[1]★ W. P. Chen,[2,3]★ J. C. Pandey,[1] Athul Dileep,[1] Zhong-Han Ai,[3] Alisher S. Hojaev,[4] Neelam Panwar,[1] Santosh Joshi,[1] Soumen Mondal,[5] Siddhartha Biswas[5] and B. C. Bhatt[6]

[1]*Aryabhatta Research Institute of Observational Sciences, Manora Peak, Nainital 263001, Uttarakhand, India*
[2]*Graduate Institute of Astronomy, National Central University, 300 Zhongda Road, Zhongli 32001 Taoyuan, Taiwan*
[3]*Department of Physics, National Central University, 300 Zhongda Road, Zhongli 32001 Taoyuan, Taiwan*
[4]*Ulugh Beg Astronomical Institute, Uzbekistan Academy of Sciences, Tashkent, Republic of Uzbekistan*
[5]*S. N. Bose National Centre for Basic Sciences, Kolkata 700106, India*
[6]*Indian Institute of Astrophysics, Koramangala, Bangalore-560034, India*

Accepted 2022 December 22. Received 2022 December 6; in original form 2022 September 29

ABSTRACT

We present stellar variability towards the young open cluster NGC 6823. Time series *V*- and *I*-band CCD photometry led to identification and characterization of 88 variable stars, of which only 14 have been previously recognized. We ascertain the membership of each variable with optical *UBVI* and infrared photometry, and with Gaia EDR3 parallax and proper motion data. Seventy two variable stars are found to be cluster members, of which 25 are main sequence stars and 48 are pre-main-sequence stars. The probable cluster members collectively suggest an isochrone age of the cluster to be about 2 Myrs based on the GAIA photometry. With the colour and magnitude, as well as the shape of the light curve, we have classified the main sequence variables into β Cep, δ Scuti, slowly pulsating B type, and new class variables. Among the pre-main-sequence variables, eight are classical T Tauri variables, and four are Herbig Ae/Be objects, whereas the remaining belong to the weak-lined T Tauri population. The variable nature of 32 stars is validated with TESS light curves. Our work provides refined classification of variability of pre-main-sequence and main-sequence cluster members of the active star-forming complex, Sharpless 86. Despite no strong evidence of the disc-locking mechanism in the present sample of TTSs, one TTS with larger $\Delta(I-K)$ is found to be a slow rotator.

Key words: open clusters and associations: individual NGC 6823 – Hertzsprung-Russell and colour-magnitude diagram – stars: pre-main-sequence – stars: variables: T Tauri – Herbig Ae/Be.

1 INTRODUCTION

Young open clusters serve as useful tools for the study of the star formation mechanism and early stellar evolution. For example, young star clusters are used to trace the Galactic spiral structure. In particular, variability of young stellar members provides diagnostics on the sporadic (accretion or occultation) or periodical (rotation) properties of the stars, and of their relation to the circumstellar environments (Morales-Calderon et al. 2011).

Pre-main-sequence (PMS) objects are categorized on the basis of the spectral energy distribution in the infrared wavelengths: Class 0, Class I, Class II, and Class III (Lada 1987; Andre, Ward-Thompson & Barsony 1993) with the classification sequence roughly corresponding to the evolutionary status. Namely, a Class 0 object signifies a clump of dust and gas heavily enshrouded in the molecular envelope, and is detected only in far-infrared wavelengths or longer. A Class I object is more evolved, now emerging from the cloud to become visible in near-infrared (NIR) and mid-infrared (MIR). A Class I object is in the protostellar stage and derives the luminosity from mass accretion.

A Class II object, corresponding to a classical T Tauri star (TTS), has dispersed much of the envelope of gas and dust but retains a circumstellar disc within which planets may condense or are being formed. Inside the optically thick but geometrically thin disc, the dust grains absorb the starlight and re-emit in the infrared, manifest as infrared excess seen typically in a classical TTS. Accretion from the disc onto the star, while matter is partly lost as bipolar jets/outflows, leads to strong emission lines in the spectrum. As the inner disc is dissipated (or going into planet formation), the PMS object then evolves to Class III, now with negligible infrared excess and with weak emission lines, if any, due to surface chromospheric activity. A Class III object hence is called a weak-lined TTS (Joy 1945; Appenzeller & Mundt 1989). Variability of PMS objects hence serves as an important diagnosis to understand the earliest PMS stellar evolution, e.g. the accretion (Johnstone et al. 2018), rotation (Herbst et al. 1994), or dust properties (Huang et al. 2019).

Here we report the variability study of the Galactic young open cluster NGC 6823. At a distance of about 2 kpc, the cluster is associated with the prominent H II region, Sharpless 86. This cluster has been investigated by several authors (Turner 1979; Sagar and Joshi 1981; Stone 1988; Guetter 1992; Massey et al. 1995; Pigulski, Kolaczkowski & Kopacki 2000; Hojaev, Chen & Lee 2003; Bica, Bonatto & Dutra 2008; Zahajkiewicz 2012). Using optical and *JHK* photometric observations, Riaz et al. (2012) found a large population of young stellar sources in the region, including two δ Scuti variables of PMS nature, and 13 other variables such as eclipsing binaries, slowly pulsating B type (SPB) candidates, and UX Ori type variables. In the

★ E-mail: sneh@aries.res.in (SL); wchen@astro.ncu.edu.tw (WPC)

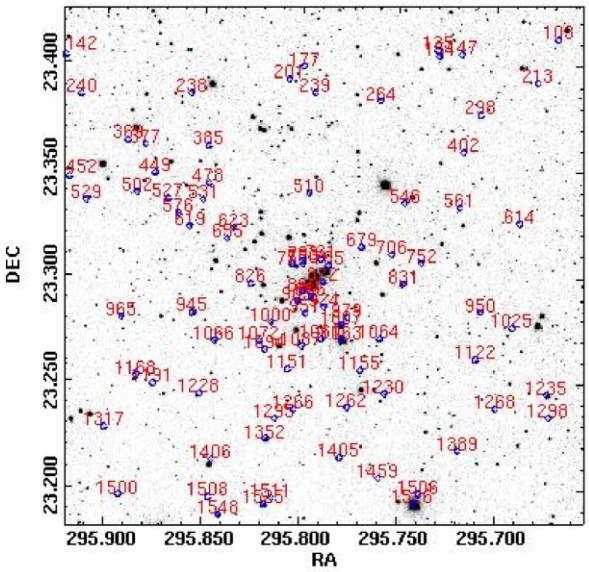

Figure 1. The observed region of open cluster NGC 6823. Each variable star identified in this work is encircled.

line of sight to the cluster the reddening has been found to be from 0.7 to 1.1 mag following a normal reddening law (Rangwal et al. 2017). The aim of the present work is to identify variables in a relatively large field of $\sim 14^{'} \times 14^{'}$ of the member versus nonmember variable stellar populations in the region. Particularly, photometric rotation periods of PMS members are derived to add to the data inventory for the study of the angular momentum evolution of low-mass stars.

We describe in Section 2 observations, data reduction procedure, detection of variables, and period determinations. In Section 3, membership of the identified variable candidates is discussed using Gaia proper motion data, photometric two-color diagrams (TCDs) and color-magnitude diagrams (CMDs). Section 4 then presents the nature of known and newly identified variable stars, while Section 5 deals with Transiting Exoplanet Survey Satellite (TESS) light curves. We discuss correlation between amplitude and rotation periods of TTSs along with their colour excess in Section 6. The results are summarized in Section 7.

2 OBSERVATIONS AND DATA REDUCTION

We have observed NGC 6823 with the 0.81-m f/7 Ritchey–Chretien Tenagra automated telescope in southern Arizona, equipped with a 1024 × 1024 pixel SITe camera. Each pixel corresponds to 0.87 arcsec, which yields a field of view of ∼14.8 arcmin × 14.8 arcmin. The observations were carried out from 2012 early October to 2012 December. In total, data were acquired on 54 nights in two passbands, with 232 frames in *V* band and 243 frames in *I* band, with typical seeing of 2–3 arcsec Bias and twilight flats were taken every observing night. The observed region of the cluster in *I* band is shown in Fig. 1. The log of the observations is given in Table 1.

The observed images were processed using standard Image Reduction and Analysis Facility (IRAF) tasks: zerocombine, flatcombine, and CCDPROC. We have performed aperture as well as point spread function (PSF) photometry to derive the magnitude of stars. The PSF photometry was obtained using program ALLSTAR (Stetson 1987). To match the stars between different photometric files we used the daomatch routine of DAOPHOT (Stetson 1992), whereas daomaster was used to match the point sources, and to obtain a

Table 1. Log of the observations of NGC 6823. *N* and Exp. represent number of frames obtained and exposure time in seconds, respectively.

S. No.	Date of Observations	*I* (*N*×Exp.)	*V* (*N*×Exp.)
1	2012 Oct 13	6 × 30	6 × 50
2	2012 Oct 15	3 × 30	3 × 50
3	2012 Oct 16	6 × 30	5 × 50
4	2012 Oct 16	6 × 30	6 × 50
5	2012 Oct 19	3 × 30	5 × 50
6	2012 Oct 20	6 × 30	6 × 50
7	2012 Oct 21	6 × 30	4 × 50
8	2012 Oct 22	6 × 30	6 × 50
9	2012 Oct 23	3 × 30	2 × 50
10	2012 Oct 24	6 × 30	6 × 50
11	2012 Oct 25	6 × 30	5 × 50
12	2012 Oct 26	5 × 30	5 × 50
13	2012 Oct 27	6 × 30	6 × 50
14	2012 Oct 28	6 × 30	6 × 50
15	2012 Oct 29	6 × 30	6 × 50
16	2012 Oct 30	6 × 30	6 × 50
17	2012 Oct 31	6 × 30	6 × 50
18	2012 Nov 01	6 × 30	4 × 50
19	2012 Nov 02	–	2 × 50
20	2012 Nov 03	6 × 30	5 × 50
21	2012 Nov 04	6 × 30	5 × 50
22	2012 Nov 05	5 × 30	5 × 50
23	2012 Nov 06	6 × 30	6 × 50
24	2012 Nov 08	6 × 30	6 × 50
25	2012 Nov 11	5 × 30	5 × 50
26	2012 Nov 12	2 × 30	3 × 50
27	2012 Nov 14	6 × 30	6 × 50
28	2012 Nov 17	3 × 30	3 × 50
29	2012 Nov 19	3 × 30	3 × 50
30	2012 Nov 20	6 × 30	6 × 50
31	2012 Nov 22	6 × 30	6 × 50
32	2012 Nov 25	6 × 30	6 × 50
33	2012 Nov 27	6 × 30	6 × 50
34	2012 Nov 28	6 × 30	6 × 50
35	2012 Nov 29	5 × 30	3 × 50
36	2012 Nov 30	6 × 30	6 × 50
37	2012 Dec 01	3 × 30	3 × 50
38	2012 Dec 02	3 × 30	3 × 50
39	2012 Dec 03	3 × 30	3 × 50
40	2012 Dec 04	3 × 30	3 × 50
41	2012 Dec 05	3 × 30	3 × 50
42	2012 Dec 06	3 × 30	3 × 50
43	2012 Dec 07	3 × 30	3 × 50
44	2012 Dec 08	3 × 30	3 × 50
45	2012 Dec 09	3 × 30	3 × 50
46	2012 Dec 10	3 × 30	1 × 50
47	2012 Dec 11	2 × 30	2 × 50
48	2012 Dec 12	3 × 30	3 × 50
49	2012 Dec 13	3 × 30	3 × 50
50	2012 Dec 17	3 × 30	3 × 50
51	2012 Dec 18	3 × 30	3 × 50
52	2012 Dec 20	3 × 30	3 × 50
53	2012 Dec 21	3 × 30	3 × 50
54	2012 Dec 26	6 × 30	–

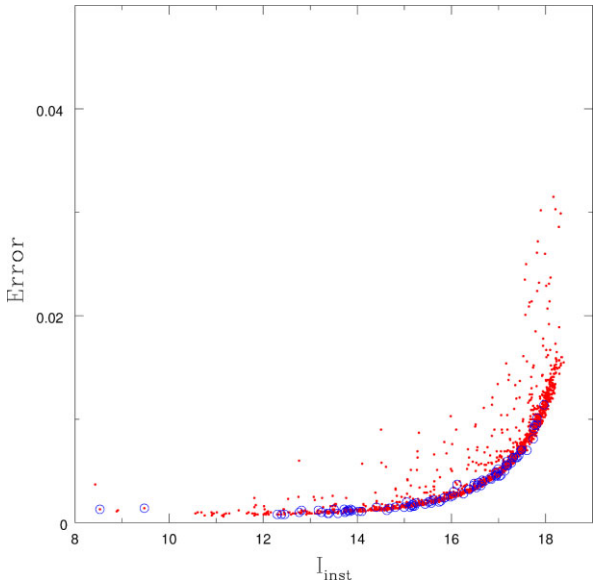

Figure 2. Photometric errors as a function of instrumental magnitude in I band. Open circles represent the variable stars identified in the present work.

file having corrected magnitude of stars from all the files. The daomaster program also removes the flux variation of stars in different frames due to exposure time and airmass. This program makes the magnitudes of stars in each photometry file equal to that of reference file by applying a constant value.

We have used the V and I observations of Massey et al. (1995) for conversion of the present instrumental magnitudes to the standard ones. For this, the mean instrumental magnitudes in V and I bands given by DAOMASTER (Stetson 1992) have been converted into standard ones with the following transformation equations.

$$V = v + (-0.042 \pm 0.001) \times (V - I) + 0.818 \pm 0.014$$
$$V - I = (0.982 \pm 0.004) \times (v - i) + 1.185 \pm 0.002,$$

where v and i are the instrumental magnitudes, and V and I refer to the standard magnitudes of stars in V and I filters. The estimated photometric error as a function of the mean instrumental magnitude is shown in Fig. 2.

2.1 Variables identification

To identify variable stars, we first produced the light curves of all the stars cross-matched in different CCD frames. The light curves were obtained by plotting the differential magnitudes (Δm) of stars (variable minus the comparison star) against the given Julian date (JD). We used the Lomb–Scargle periodogram (Lomb 1976; Scargle 1982) to derive the periods and produced phased light curves accordingly to ascertain their most probable periods. A few variables seem to show periodic variability but their periodic nature was not obvious in their observed light curves. The phased light curves of all stars were inspected, and we adopted the period value which produces the most consistent phased light curve. The light curves of a few variables are shown in Fig. 3 as examples. The phased light curves of variables identified in both V and I bands are presented in Figs 4 and 5, whereas Fig. 6 shows variables identified in the I band only.

By eye inspection and periodogram analysis, we have detected 88 variables. We have listed optical and NIR data of the variable stars in Table 2, including an identification number, coordinates, and optical as well as NIR photometric data. These are the star ID numbers

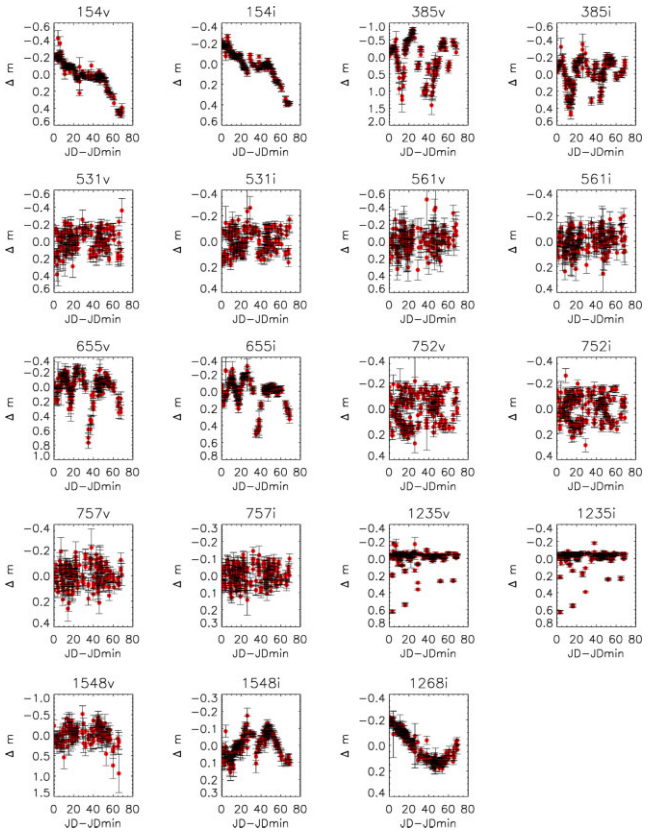

Figure 3. The V and I band sample light curves of a few variables identified in the present work where Δm represents the differential magnitude.

labelled in Fig. 1. These 88 variable stars include 14 known variables, with periods varying from ∼0.03 days to more than 60 days. We have plotted in Fig. 7 the root mean square (RMS) scatter of each star to confirm their variability. The observed RMS scatter includes both the intrinsic variability and the mean photometric error. The larger circles in Fig. 7 show the variables identified in the present work, indicating large RMS values for variables. Some stars have large RMS values but do not show noticeable brightness variation. Some of these objects are found to be close to the edge of the detector, whereas a few stars contain spurious data points. The derived periods of stars are given in Table 2.

3 CLUSTER MEMBERSHIP OF VARIABLE STARS

For each variable star, its *UBVI* plus 2MASS photometry along with Gaia EDR3 proper motion and parallax (Gaia Collaboration 2016, 2021) have been used to assess the likelihood of cluster membership. The *UBV*, *JHK*, and MIR data at wavelengths 3.6, 4.5, 5.8, and 8 micron are taken from Massey et al. (1995), Cutri et al. (2003), and GLIMPSE survey, respectively.

3.1 Gaia Characterization of the Variable Stars

The 88 variable stars reported in this work have been characterized with the Gaia EDR3 parallax and proper motion measurements. Fig. 8 plots the sky positions of all the Gaia sources (in gray) within 30 arcmin towards NGC 6823. This covers the field of the Tenagra images (variable stars marked in black crosses) and is much wider

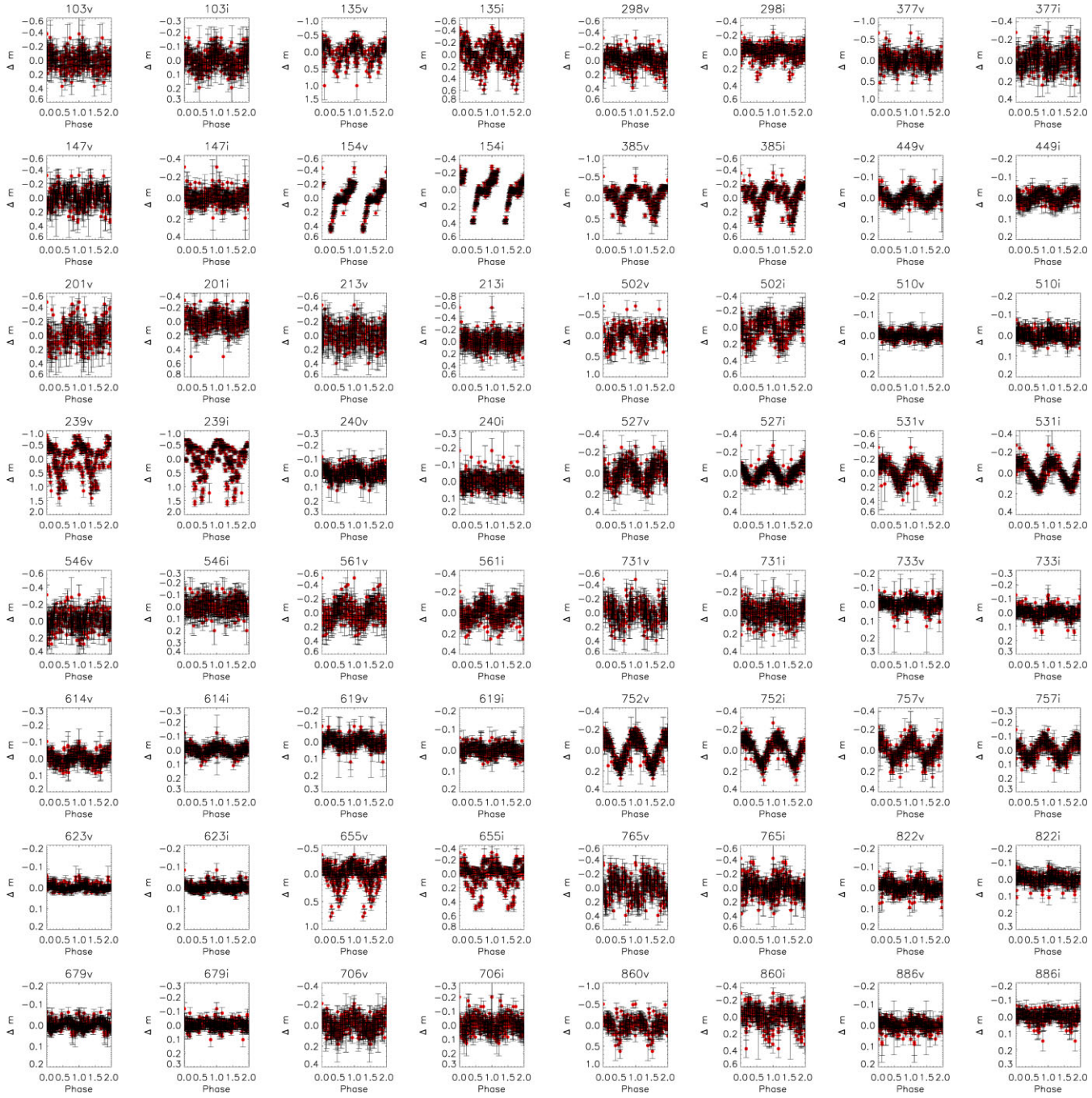

Figure 4. The *I* and *V* band phased light curves of variable stars identified in the region of NGC 6823.

than the cluster's angular size of ∼3′.6 (red circle) (Morales et al. 2013). The stellar density is clearly enhanced towards the centre.

Each variable star was matched with Gaia counterparts within a radius of 2.5 arcsec as the compromise of the seeing of the Tenagra images, leading to 91 Gaia sources. Fig. 9 presents the proper motion vector plot of all the stars (gray) and those within 4 arcmin nominal cluster region (black small circles, 1294 stars) for which the members should be concentrated, serving as the sample of cluster members. This 4 arcmin (positional) sample has a mean of $\mu_\alpha \approx -1.7$ mas yr^{-1} and $\mu_\delta \approx -5.3$ mas yr^{-1}, which agrees well with the literature values (Cantat-Gaudin & Anders 2020). Shown in the bottom panel are the proper motions for variable stars (in black with error bars). One sees that the majority of our variable stars share the same proper motion ranges.

Gaia measures repeatedly the astrometry of a source from which the parallax and proper motion are solved simultaneously. Parallax, however, does not serve as a constraint for membership as stringently as the proper motion, because given the uncertainties, negative average values may result, rendering the reciprocal to estimate the distance possible only if a statistical inference is exercised (Bailer-Jones et al. 2021). For our work, the parallax value was used directly. The parallax of the 4 acrmin sample exhibits a peak around 0.45 mas, indeed consistent with the literature value (Cantat-Gaudin & Anders 2020), and so does the variable star sample, as demonstrated in

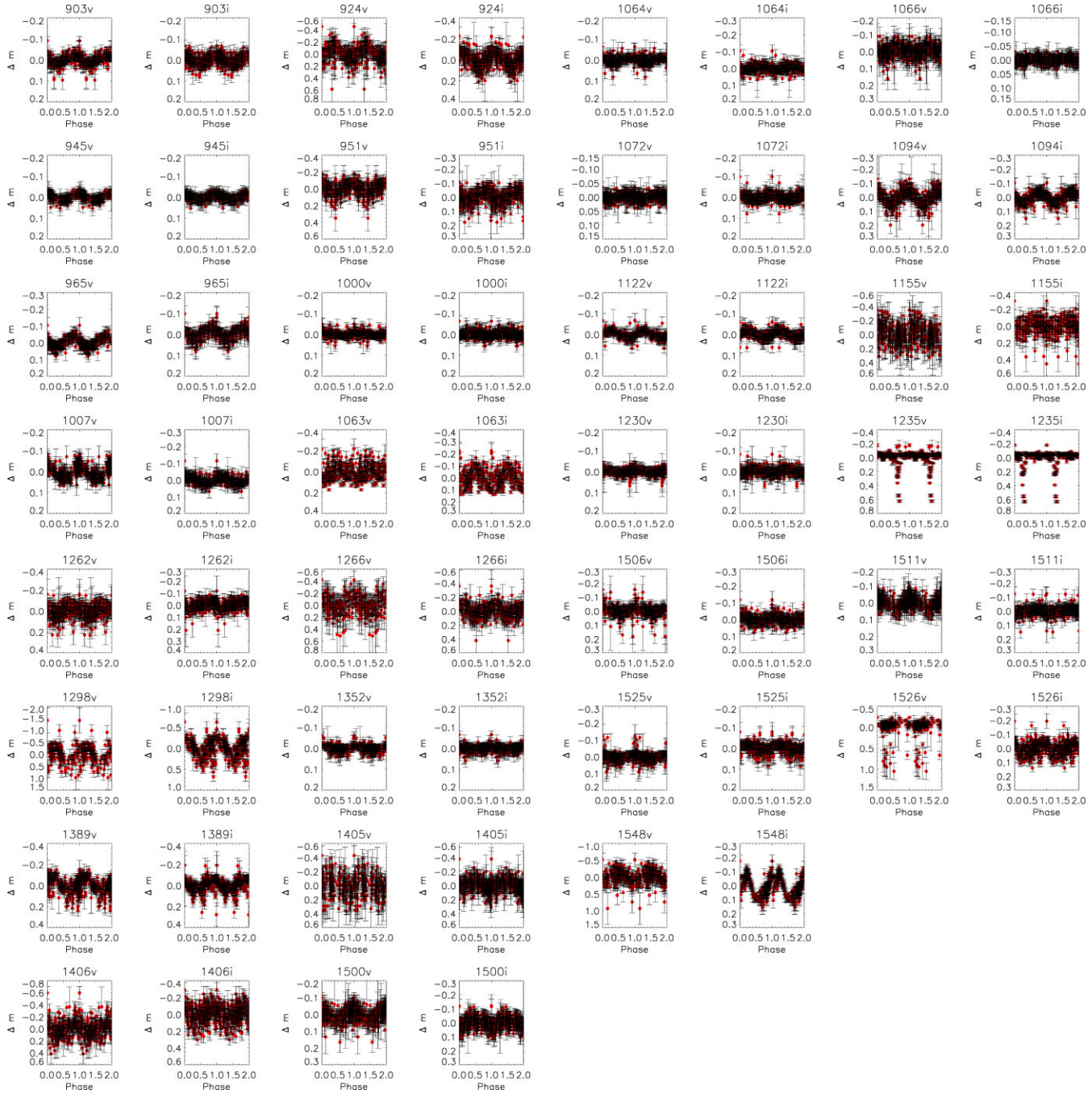

Figure 5. The I and V band phased light curves of variable stars identified in the region of NGC 6823.

Fig. 10. If the 4 acrmin sample is further divided by proper motion ranges, one finds no star within 1–2 mas yr^{-1} from the cluster's mean having parallax between 0.4 mas and 0.6 mas. This signifies the sufficiency as membership criteria of (1) a radius of 1 mas yr^{-1} in the proper motion from the cluster average proper motion, and (2) a parallax value of 0.35–0.55 mas. A variable satisfying both (1) and (2) is therefore considered a 'highly probable' member, whereas one that fulfils only (1) or (2) is classified as a 'possible' member. Table 3 lists information about the proper motions, parallax, and magnitudes for the 88 variables identified in the present work.

Fig. 11 shows the Gaia G versus $BP - RP$ CMD for the highly probable members (in red) and possible members (in blue). Overlapped in the diagram is the PARSEC isochrones of 1, 2, and 4 Myr, respectively, each shifted by a distance modulus of 11.753 (parallax of 0.446 mas) and reddening of $E(B-V) = 0.8$ (Sagar & Joshi 1981) adopting the reddening law of $A_V = 3.1\,E(B-V)$, $A_G = 0.83627\,A_V$, $A_{BP} = 1.08337\,A_V$, and $A_{RP} = 0.63439\,A_V$. The highly probable members indicate an age of roughly 2 Myr.

Three variables have ambiguous Gaia counterparts within the matching radius. Star No. 478 has two possible matches, equally faint thereby with relatively large uncertainties in Gaia data, but either one is consistent with being a member. The star was not detected in our V band image and appears progressively brighter from $I = 14.47$ mag, to 2MASS $J = 13.42$ mag, $H = 13.42$ mag, and $Ks = 13.00$ mag.

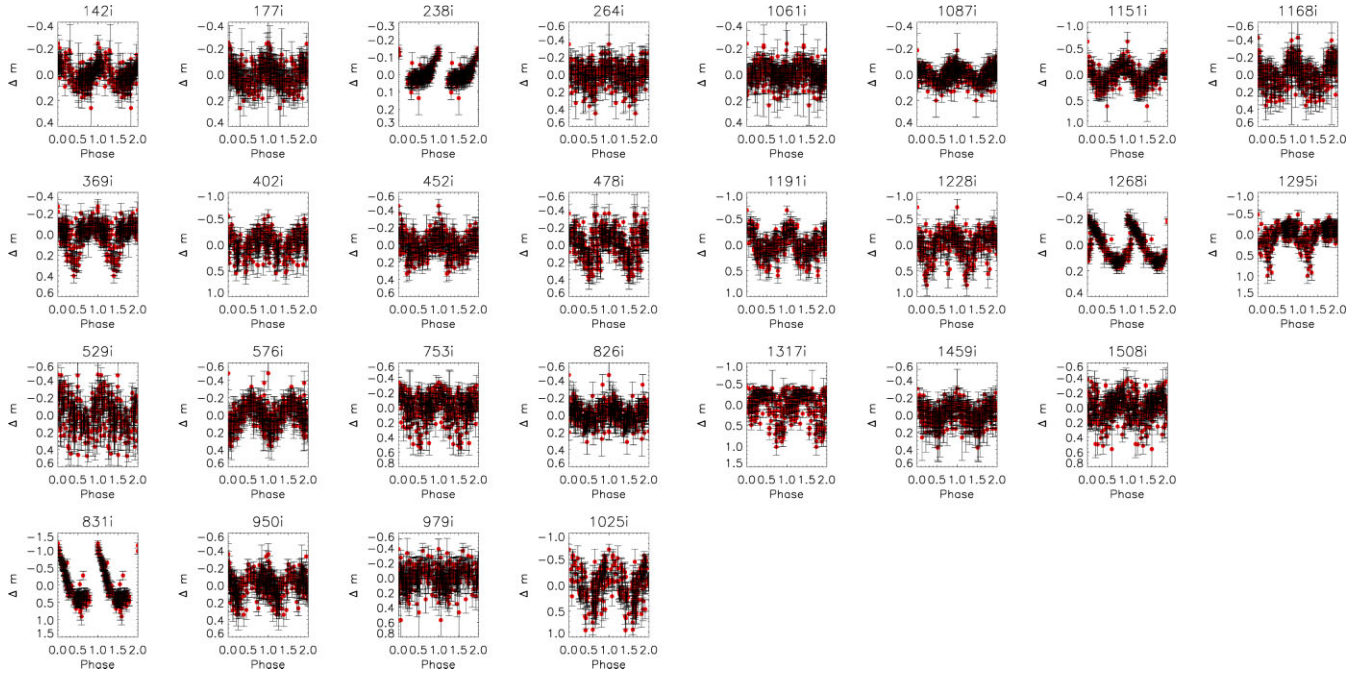

Figure 6. The *I* band phased light curves of probable variable candidates around the cluster.

Star No. 1063 is the second brightest star in our variable list, with the brightest one (No. 1526) being clearly not a member. The star also has two Gaia matches, with contrasting brightness (G = 9.72 mag versus 12.87 mag). Given its $V = 9.70$ mag, the fainter one, having an outlying parallax of 0.282 mas, is eliminated. The other counterpart, however, has a negative parallax value with a large uncertainty. This compromises its membership determination. Its optical and NIR colours both suggest an early-type star and its position in the CMD suggests a main-sequence member.

Star No. 1262 has $V = 17.173$ mag, 2MASS $J = 13.351$ mag, $H = 12.474$ mag, and $Ks = 11.998$ mag. The brighter Gaia match has $G = 16.379$ mag but has a negative parallax value and inconsistent proper motion. The other Gaia star is faint, with $G = 19.291$, and no measurement in the other two Gaia bands has parallax and proper motion values well consistent with being a member.

3.2 Colours and Magnitudes

3.2.1 U − B vs B − V TCD

To identify probable main-sequence (MS) variables, we have plotted in Fig. 12 the $U - B$ versus $B - V$ for variable stars identified in the cluster region with the photometric data of 22 stars found in Massey et al. (1995). Reddening in terms of colour excess $E(B - V)$ ranges from 0.7 to 1.1 mag (Erickson 1971; Guetter 1992; Massey et al. 1995; Pigulski et al. 2000). Pigulski et al. (2000) recognized the highest extinction in the eastern part of the cluster where a trapezium system, i.e. of O, B spectral types, is located. The eastern part of their observed field is the direction to the reflection nebula NGC 6820, and their study suggested more than half of the total absorption to arise from nearby interstellar matter towards NGC 6823. It is inferred that there is a significant differential reddening within the cluster, manifest that the cluster is located behind at least $A_V = \sim 3$ mag (Riaz et al. 2012). Rangwal et al. (2017) studied the interstellar extinction of open clusters and found that NGC 6823 follows a normal extinction law in optical as well as in the NIR wavelengths. The $U - B$ versus $B - V$ TCD shows that the stars exhibiting within $E(B - V) = 0.7$–1.1 mag could be MS members of the cluster, indicating a nonuniform reddening across the cluster. The reddened theoretical zero-age main sequence (ZAMS) of Girardi et al. (2002) is fitted to the TCD. The value of colour excess $E(V - I)$ was taken as 0.88 mag, which has been calculated using the minimum reddening value of $E(B - V) = 0.70$ mag.

3.2.2 J − H vs H − K TCD

Fig. 13 shows the $J - H$ versus $H - K$ TCD for NGC 6823. Only 86 stars were cross-matched between the present sample of variable stars and the 2MASS catalog, with the *JHK* counterparts of two stars No. 201 and No. 377 not found during the match. In the 2MASS TCD, the 'F' and 'T' regions are locations of probable Class III/field stars and Class II sources, respectively. The filled squares plotted in blue and green colours represent, respectively, probable PMS and MS members. Circles in the diagram represents field stars. Riaz et al. (2012) from their NIR CCD found early-type MS dwarfs concentrating close to $(H - Ks) \sim 0.7$ mag, and $(J - H) \sim 1.5$ mag, having extinction $A_V \geq 10$. These authors have noticed another population near the classical TTS locus close to $(H - Ks) \sim 0.6$ mag and $(J - H) \sim 1.0$ mag, presumably being young disc-bearing members. In the 2MASS TCD, about half the detected variables are in the 'T' or 'F' regions, hence could be T Tauri variables. A few PMS stars located below the TTS locus are probably Herbig Ae/Be stars. We note that star No. 679 occupies the position where Herbig Ae/Be stars are placed, while in $U - B$ versus $B - V$ TCD, it lies close to the MS locus; it could thus be either a reddened MS star or a Herbig Ae/Be member.

Following Gutermuth et al. (2008) to classify young stellar sources, Riaz et al. (2012) used MIR IRAC data and found 2 Class I, 94 Class II, and 394 Class III or field stars in the region. The fig. 4(a) of Riaz et al. (2012) is plotted with the $(H - Ks)$ and [4.5] − [8] TCD for the 490 sources. This shows both YSOs and the discless

Table 2. The *VI* and *JHK* 2mass data, amplitude, and period of variables identified towards NGC 6823. The 2MASS data were obtained from the 2mass catalogue (Cutri et al. 2003). The first column with an asterisk symbol represents a known variable.

ID	RA	Dec	V (mag)	$V-I$ (mag)	J (mag)	H (mag)	K (mag)
103	295.668444	23.412417	18.115 ± 0.101	2.190 ± 0.048	14.231 ± 0.041	13.140 ± 0.036	12.508 ± 0.034
135	295.730111	23.406833	18.454 ± 0.124	2.428 ± 0.054	14.324 ± 0.056	12.758 ± 0.081	11.586 ± 0.044
142	295.921528	23.403194	–	–	9.997 ± 0.022	8.072 ± 0.034	7.137 ± 0.020
147	295.717833	23.404972	18.251 ± 0.102	2.442 ± 0.043	13.925 ± 0.029	12.915 ± 0.037	12.452 ± 0.031
154	295.729444	23.404194	15.305 ± 0.021	2.514 ± 0.015	10.509 ± 0.021	9.561 ± 0.030	8.621 ± 0.024
177	295.798972	23.398806	–	–	14.623 ± 0.040	13.622 ± 0.040	13.154 ± 0.036
201	295.806361	23.392806	18.651 ± 0.129	1.686± –	–	–	–
213	295.678611	23.391889	18.583 ± 0.133	1.531 ± 0.099	15.949 ± 0.093	15.302 ± 0.128	14.913 ± 0.129
238	295.856583	23.385806	–	–	9.096 ± 0.022	7.248 ± 0.033	6.386 ± 0.027
239	295.793083	23.386500	17.564 ± 0.063	2.161 ± 0.036	13.328± –	12.411 ± 0.044	11.853 ± 0.034
240	295.913278	23.384861	16.320 ± 0.033	1.113 ± 0.034	14.480 ± 0.035	14.178 ± 0.051	14.074 ± 0.052
264	295.759250	23.382944	–	–	14.953 ± 0.040	14.097 ± 0.043	13.771 ± 0.045
298	295.707806	23.376667	17.367 ± 0.056	1.772 ± 0.040	14.216 ± 0.034	13.319 ± 0.040	12.605 ± 0.030
369	295.889056	23.363222	–	–	13.520 ± 0.026	12.672 ± 0.033	12.243 ± 0.031
377	295.880000	23.361417	18.610 ± 0.127	2.027± –	–	–	–
385	295.847556	23.360861	16.904 ± 0.040	1.763 ± 0.029	13.554 ± 0.028	12.719 ± 0.033	12.086 ± 0.027
402	295.716611	23.358944	–	–	15.213 ± 0.058	14.159 ± 0.063	13.558 ± 0.056
449	295.874806	23.347806	14.985 ± 0.017	1.571 ± 0.017	12.262 ± 0.023	11.665 ± 0.028	11.521 ± 0.024
452	295.918972	23.345917	–	–	14.529 ± 0.056	13.475 ± 0.055	13.008 ± 0.043
478	295.847167	23.343222	–	–	14.474 ± 0.042	13.418 ± 0.046	13.002 ± 0.043
502	295.883889	23.339000	18.593 ± 0.122	2.086 ± 0.067	15.050 ± 0.051	14.019 ± 0.053	13.695 ± 0.055
510	295.795694	23.339139	14.154 ± 0.014	1.061 ± 0.020	12.211 ± 0.021	11.957 ± 0.031	11.770 ± 0.027
527	295.868056	23.335778	17.461 ± 0.055	2.126 ± 0.032	13.688 ± 0.037	12.840 ± 0.040	12.605 ± 0.038
529	295.910194	23.335083	–	–	14.243 ± 0.039	12.844 ± 0.040	11.984 ± 0.033
531	295.850028	23.335583	17.400 ± 0.055	2.102 ± 0.031	13.562 ± 0.032	12.740 ± 0.036	12.460 ± 0.031
546	295.746583	23.334750	17.928 ± 0.082	1.702 ± 0.060	14.461± –	13.676± –	14.144 ± 0.102
561	295.718194	23.332694	18.193 ± 0.100	2.100 ± 0.051	14.652± –	13.775± –	13.376 ± 0.041
576	295.862722	23.329111	–	–	14.668 ± 0.042	13.423 ± 0.039	12.865 ± 0.034
614	295.687444	23.325333	15.851 ± 0.023	1.277 ± 0.023	13.709 ± 0.028	13.328 ± 0.041	13.109 ± 0.036
619	295.856806	23.323000	15.920 ± 0.022	1.721 ± 0.018	12.883 ± 0.024	12.309 ± 0.031	12.076 ± 0.026
623*	295.834472	23.322306	13.173 ± 0.009	1.202 ± 0.012	11.141 ± 0.019	10.662 ± 0.030	10.519 ± 0.024
655*	295.837528	23.317306	17.282 ± 0.052	2.287 ± 0.028	12.735 ± 0.025	11.397 ± 0.031	10.313 ± 0.023
679	295.768611	23.313583	13.725 ± 0.014	0.967 ± 0.018	11.556 ± 0.021	10.530 ± 0.030	9.546 ± 0.024
706	295.752944	23.310389	17.376 ± 0.056	1.963 ± 0.036	13.936 ± 0.037	13.149 ± 0.046	12.880 ± 0.041
731	295.789306	23.307667	18.493 ± 0.128	2.239 ± 0.060	14.424 ± 0.043	13.458 ± 0.051	13.086 ± 0.044
733*	295.798444	23.307361	15.211 ± 0.018	1.224 ± 0.023	12.935 ± 0.029	12.515 ± 0.045	12.256 ± 0.044
752	295.737667	23.306472	16.172 ± 0.028	1.398 ± 0.028	13.743 ± 0.028	13.207 ± 0.040	12.978 ± 0.037
753*	295.798472	23.305694	–	–	14.578 ± 0.048	13.491 ± 0.062	12.736 ± 0.058
757*	295.803833	23.305278	16.899 ± 0.042	2.077 ± 0.029	13.186 ± 0.028	12.420 ± 0.035	12.138 ± 0.031
765	295.785417	23.304806	17.592 ± 0.124	1.533 ± 0.075	14.421± –	14.039 ± 0.103	13.848 ± 0.076
822*	295.787917	23.297000	14.529 ± 0.015	1.225 ± 0.020	12.396 ± 0.026	12.024 ± 0.030	11.823 ± 0.032
826	295.825139	23.295944	–	–	14.661 ± 0.044	13.740 ± 0.051	13.406 ± 0.045
831*	295.746556	23.296667	–	–	11.266 ± 0.033	8.761 ± 0.030	7.326 ± 0.020
860	295.798389	23.292583	17.563 ± 0.121	1.880 ± 0.072	14.754 ± 0.055	13.748 ± 0.045	13.055 ± 0.041
886*	295.794056	23.290250	14.448 ± 0.015	1.065 ± 0.018	12.637 ± 0.022	12.379 ± 0.031	12.207 ± 0.029
903*	295.801167	23.288028	14.382 ± 0.014	1.036 ± 0.017	12.568± –	12.141± –	11.928 ± 0.033
924*	295.787583	23.285444	18.146 ± 0.097	2.210 ± 0.048	14.154± –	13.363± –	13.035 ± 0.046
945	295.855139	23.282167	14.524 ± 0.014	1.206 ± 0.015	12.395 ± 0.033	12.051 ± 0.040	11.913 ± 0.033
950	295.707250	23.283611	–	–	12.424 ± 0.022	11.060 ± 0.026	10.310 ± 0.021
951	295.797167	23.282278	17.150 ± 0.051	2.019 ± 0.032	13.664 ± 0.030	12.913 ± 0.043	12.626 ± 0.038
965	295.891500	23.279944	14.600 ± 0.017	1.125 ± 0.018	12.661 ± 0.023	12.150 ± 0.031	12.050 ± 0.030
979*	295.775389	23.280333	–	–	15.201 ± 0.083	14.179 ± 0.079	13.432 ± 0.057
1000	295.814639	23.277861	13.574 ± 0.011	0.579 ± 0.014	12.544 ± 0.021	12.472 ± 0.033	12.342 ± 0.032
1007*	295.778417	23.277111	14.624 ± 0.016	1.181 ± 0.020	12.508 ± 0.026	12.220 ± 0.039	12.003 ± 0.033
1025	295.690889	23.276194	–	–	15.839 ± 0.088	14.503 ± 0.058	13.751 ± 0.052
1061*	295.788972	23.270083	–	–	14.267 ± 0.033	12.456± –	12.081± –
1063	295.778528	23.270139	9.702 ± 0.018	0.631 ± 0.018	8.785 ± 0.019	8.712 ± 0.029	8.652 ± 0.024
1064	295.758861	23.270389	14.451 ± 0.014	1.047 ± 0.018	12.514 ± 0.022	12.088 ± 0.035	11.874 ± 0.029
1066	295.843528	23.269278	16.715 ± 0.037	3.602 ± 0.014	10.303 ± 0.022	9.170 ± 0.028	8.693 ± 0.025
1072	295.820667	23.269139	14.714 ± 0.014	1.098 ± 0.017	12.751 ± 0.022	12.523 ± 0.033	12.317 ± 0.030
1087*	295.798806	23.266806	–	–	9.945 ± 0.019	7.952 ± 0.042	7.059 ± 0.040
1094	295.817722	23.265111	16.634 ± 0.034	1.949 ± 0.023	13.251 ± 0.022	12.572 ± 0.031	12.283 ± 0.029

Table 2 – *continued*

ID	RA	Dec	V (mag)	$V-I$ (mag)	J (mag)	H (mag)	K (mag)
1122	295.709611	23.261028	13.788 ± 0.011	0.824 ± 0.014	12.308 ± 0.022	12.085 ± 0.032	11.956 ± 0.028
1151	295.806028	23.255889	–	–	15.007 ± 0.059	13.956 ± 0.041	13.596 ± 0.046
1155	295.768556	23.255472	18.407 ± 0.117	2.004 ± 0.062	14.928 ± 0.039	14.169 ± 0.049	13.918 ± 0.055
1168	295.883528	23.252556	–	–	15.273 ± 0.057	14.244 ± 0.061	13.974 ± 0.059
1191	295.875000	23.248667	–	–	15.444 ± 0.065	13.630± –	12.955± –
1228	295.851056	23.243861	–	–	15.146 ± 0.055	13.810 ± 0.063	13.109 ± 0.038
1230	295.756194	23.244750	14.580 ± 0.014	0.897 ± 0.017	12.948 ± 0.026	12.700 ± 0.036	12.604 ± 0.033
1235	295.672972	23.244722	12.983 ± 0.012	0.937 ± 0.012	11.555± –	11.322± –	11.205 ± 0.037
1262	295.775250	23.238000	17.173 ± 0.050	2.100 ± 0.030	13.351 ± 0.034	12.474 ± 0.041	11.998 ± 0.032
1266	295.802833	23.236806	18.656 ± 0.134	2.123 ± 0.069	14.808 ± 0.038	14.078 ± 0.049	13.694 ± 0.045
1268	295.699250	23.237972	–	–	9.148 ± 0.019	7.211 ± 0.034	6.303 ± 0.026
1295	295.812361	23.232472	–	–	14.982 ± 0.043	13.783 ± 0.040	12.963 ± 0.032
1298	295.671972	23.234000	18.572 ± 0.133	2.430 ± 0.059	14.280 ± 0.049	13.287 ± 0.055	12.611 ± 0.042
1317	295.899889	23.227722	–	–	15.778 ± 0.081	14.299 ± 0.063	13.344 ± 0.038
1352	295.816861	23.222944	12.586 ± 0.011	0.693 ± 0.012	11.411 ± 0.022	11.168 ± 0.030	11.106 ± 0.026
1389	295.718444	23.218000	16.432 ± 0.031	1.683 ± 0.025	13.25 ± 0.027	12.387 ± 0.034	11.659 ± 0.027
1405	295.778889	23.214194	18.752 ± 0.142	1.817 ± 0.090	15.644 ± 0.069	14.713 ± 0.071	14.516 ± 0.090
1406	295.844722	23.213083	17.981 ± 0.088	1.589 ± 0.063	15.113 ± 0.122	14.442 ± 0.237	13.856 ± 0.283
1459	295.758944	23.204833	–	–	15.208 ± 0.056	14.355 ± 0.055	13.932 ± 0.060
1500	295.892056	23.195889	15.993 ± 0.033	1.365 ± 0.031	13.631 ± 0.038	13.176 ± 0.051	13.053 ± 0.042
1506	295.738167	23.197333	15.499 ± 0.024	1.237 ± 0.021	13.540 ± –	13.123 ± 0.036	13.088± –
1508	295.846250	23.195111	–	–	14.502 ± 0.043	13.425 ± 0.050	12.769 ± 0.036
1511	295.813722	23.194889	16.513 ± 0.034	1.795 ± 0.026	13.734 ± 0.028	13.124 ± 0.037	12.874 ± 0.033
1525	295.817722	23.191972	13.517 ± 0.015	1.170 ± 0.015	11.520 ± 0.023	11.221 ± 0.028	11.071 ± 0.026
1526	295.740750	23.192917	8.846 ± 0.024	0.721 ± 0.019	7.610 ± 0.029	7.327 ± 0.036	7.256 ± 0.024
1548	295.840667	23.186917	18.460 ± 0.141	6.181 ± 0.018	8.177 ± 0.023	6.609 ± 0.017	5.875 ± 0.020

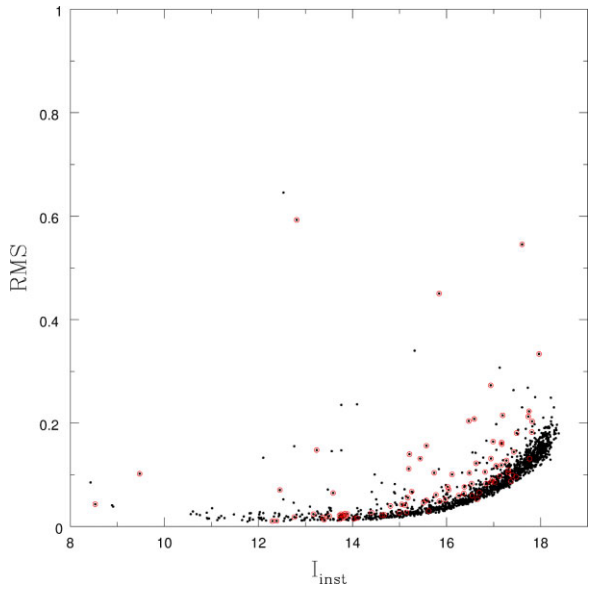

Figure 7. Magnitude as a function of *rms* value of each star detected in *I* band. Open circles represent variable stars identified in this work.

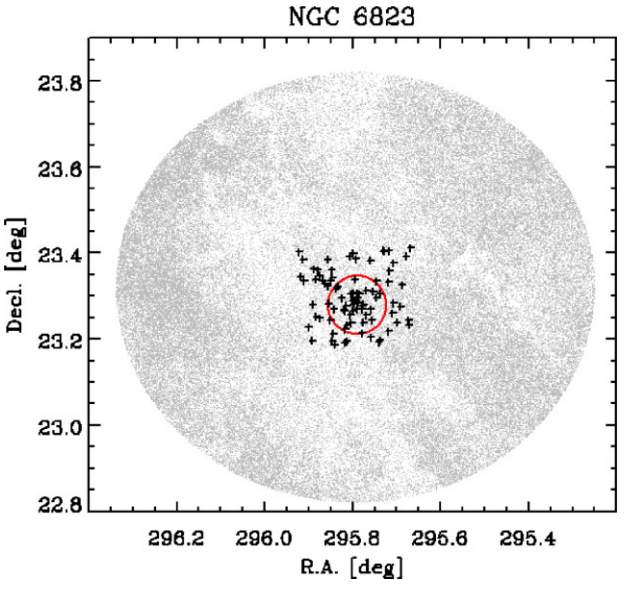

Figure 8. The sky positions of all the Gaia sources (in gray) within 30 arcmin towards NGC 6823.

sources to have similar NIR colours, but from their IRAC TCD the photospheric and the disc population at IRAC colour [4.5] − [8] ∼ 0.4 mag are readily distinguishable. They have noted that a few Class III/field stars are mixed with Class II sources. Their IRAC TCD in Fig. 4(b) shows different locales of Class I and Class II sources. The protostars (Class I) are located in the top-right corner and exhibit the reddest in the [3.6] − [5.8] colour, whereas the Class II sources are placed at [4.5] − [8] ≥ 0.5 mag, [3.6] − [5.8] ≥ 0.4 mag, and the Class III/field stars are found to be near [4.5] − [8] and [3.6] − [5.8] ∼ 0.2 to 0.3 mag.

3.2.3 NIR and MIR TCDs

To see the distribution of young variable sources, we have plotted them in the NIR and MIR TCD (left panel) and MIR TCD (right panel) in Fig. 14. To obtain these plots, we have cross-matched

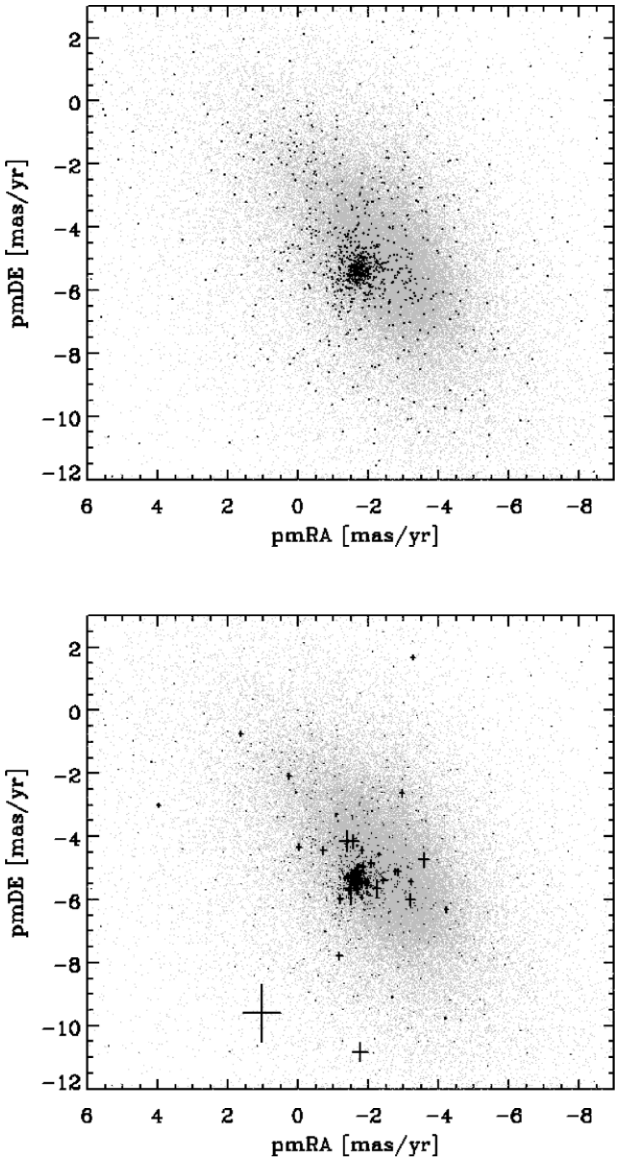

Figure 9. The upper panel represents proper motion of all the stars (gray) and those within 4 arcmin cluster region (black small circles, 1294 stars). The lower panel shows proper motions for variable stars (in black with error bars).

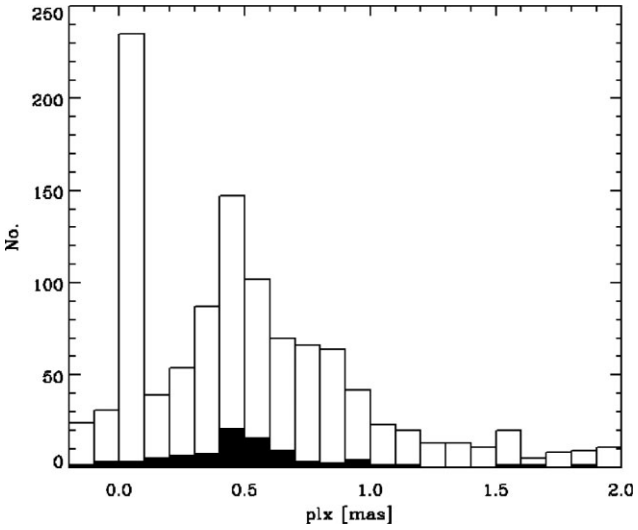

Figure 10. Histogram of parallaxes for stars within 4 arcmin, where histogram shaded with black is for variable samples identified in the present work.

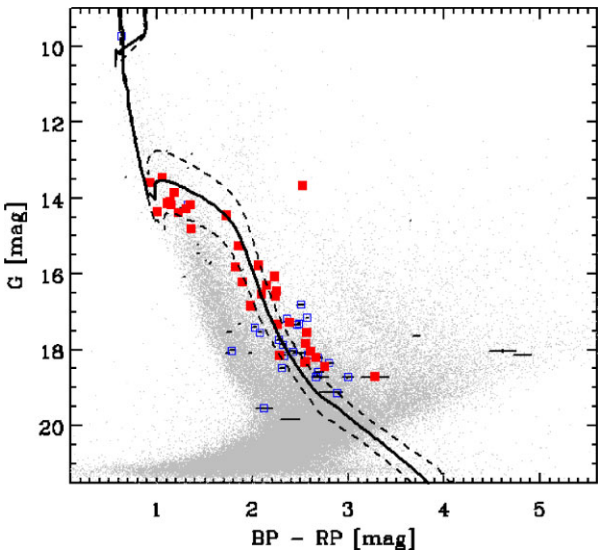

Figure 11. The G vs $BP - RP$ CMD for the present sample of variable stars. The filled and open squares denote probable and possible cluster members, and dotted points are considered nonmembers.

the coordinates of variable stars with those from the Spitzer Galactic Legacy Infrared Mid-Plane Survey Extraordinaire (GLIMPSE), yielding MIR counterparts of all 88 variable stars. A few stars, namely Nos. 154, 238, 313, 1405, and 1406 do not have magnitudes at [4.5] and other wavelengths. The $H - K$ versus [4.5] − [8] TCD shows most young stellar sources to have $H - K \gtrsim 0.3$ mag, whereas the [4.5] − [8] and [3.6] − [5.8] TCD shows a few young stellar objects to be positioned as field stars or other populations.

3.2.4 IPHAS data

To identify the young stellar sources with H_α emission, i.e. the indicator of accretion discs, we have compared the present data with Table 4 for INT Photometric Hα Survey (IPHAS) photometry of Riaz et al. (2012). We got 29 common stars after the match that have IPHAS photometry, with stars No. 502, 576, 655, 679, and 979 having H_α emission with equivalent width greater than 10 Å, judged by the $(r' - i')$ versus $(r' - H_{\rm alpha})$ TCD for NGC 6823 (Riaz et al. 2012). The location of these five stars is shown with the red square in the present $(J - H)$ versus $(H - K)$ TCD. The H_α emission is found to be variable in nature; therefore, it is necessary to check the location of the objects in spectral type/colour versus magnitude diagram to know their membership and nature (Martín et al. 2000). Two stars, Nos. 655 and 979, could be considered as PMS objects that may possess circumstellar accreting disc. Barrado y Navascués et al. (2001) showed that H_α emission depends on the spectral type or colour in the sense that H_α emission is found to be larger for cooler objects in a plot between the H_α emission and $(I - J)$ colour. The $(I - J)$ and $(I - K)$ colours for star no. 655 is about 2.26 mag and 4.682 mag, respectively. In the case of star no. 979, we have taken I magnitude from Pigulski et al. (2000) to determine its $(I - J)$ and $(I$

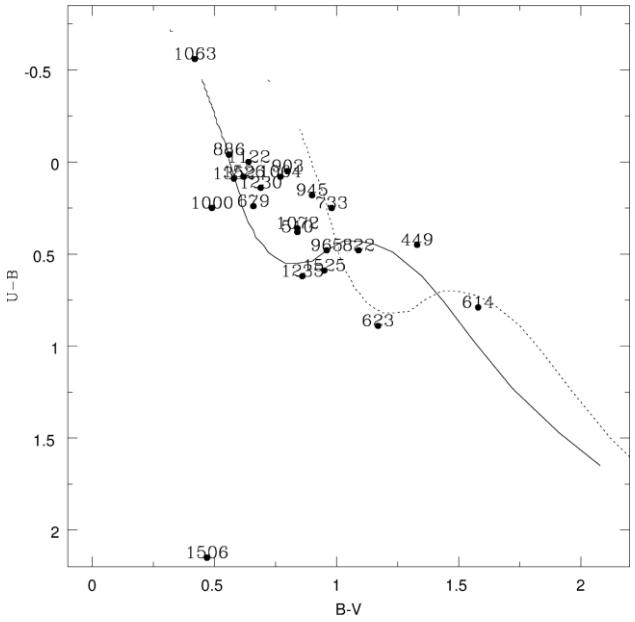

Figure 12. $(U-B)/(B-V)$ TCD for variable stars identified in the present study. All the *UBV* data are taken from Massey et al. (1995). The continuous and dotted line represent the ZAMS (Girardi et al. 2002) which are shifted along the reddening vector for reddening $E(B-V) = 0.32$ mag and 0.45 mag. Triangles are those stars that are identified as MS variables.

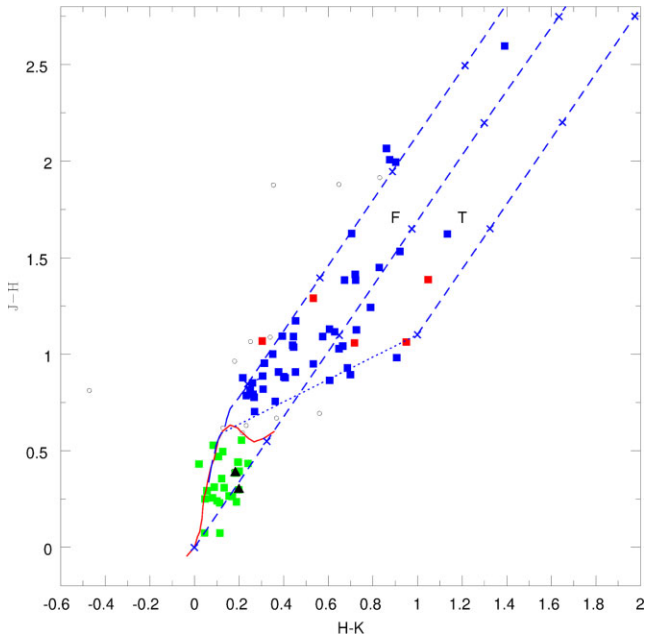

Figure 13. $(J-H)/(H-K)$ TCD for variable stars detected in the field of NGC 6823. The *JHK* data have been taken from the 2MASS catalog (Cutri et al. 2003). The continuous and long dashed lines show sequences for dwarfs and giants (Bessell & Brett 1988), respectively. The TTS locus (Meyer, Calvet & Hillenbrand 1997) is shown by a dotted line. The small dashed lines are reddening vectors (Cohen et al. 1981) and an increment of visual extinction of $A_V = 5$ mag is denoted by crosses on the reddening vectors. Filled squares with blue colours represents PMS. The MS population are shown by green squares, whereas open circles may be either MS members of the cluster or field stars. Triangles (black) represent two MS members BL 50 and HP 57.

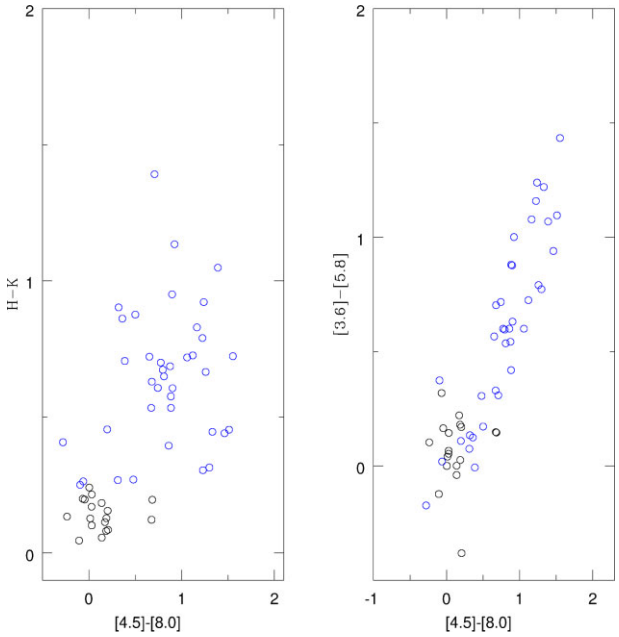

Figure 14. $(H-K)$ vs [4.5] − [8.0] and [3.6] − [5.8] vs [4.5] − [8.0] TCDs for variable stars detected in the field of NGC 6823. Blue circles are PMS young stellar sources while black circles are MS/field stars.

$-K$) colours due to lack of $(V-I)$ colour in present observations, yielding $(I-J)$ and $(I-K)$ colours as 2.020 mag and 3.789 mag, respectively. Star Nos. 655 and 979, in particular, satisfy both colours and H_α emission being greater than 10 Å; hence, these are young stars with accretion discs.

3.2.5 V vs V − I CMD

Sixty one variable stars were detected in both V and I bands. Their V magnitudes and $V-I$ colour are given in Table 2, and Fig. 15 shows their V versus $(V-I)$ CMD. The PMS isochrones and evolutionary tracks for different masses are taken from Siess, Dufour & Forestini (2000). The solid curve represents ZAMS by Girardi et al. (2002). We determined the distance modulus of the cluster to be $(V-M_V) = 14.31$ mag by comparing the ZAMS of Girardi et al. (2002) for solar metallicity to the V versus $V-I$ CMD, which corresponds to a distance of 2.59 kpc. The present estimate of distance matches well with those derived in earlier works of NGC 6823. The isochrone of age 4 Myr also fits the data well. The CMD is known to be contaminated by the foreground field stars (e.g. Guetter 1992; Pigulski et al. 2000; Bica et al. 2008). After analysis of CMD, Pigulski et al. (2000) and Riaz et al. (2012) noted two different populations in the cluster, one consisting of older, massive stars that are located near or on the ZAMS, while the other one being younger objects with ages less than 10 Myr and are of lower masses (∼0.1–0.4 $M_\odot$), that is, of PMS stars. Pigulski et al. (2000) also concluded that stars lying in B region of their Fig. 11(a) are cluster stars of PMS nature, evolving towards the MS. The present CMD containing variable stars also shows MS of the cluster to go up to around $V = 16$ mag; location of variables in the CMD suggests the majority of these stars to be probable members. Most of the fainter and redder stars lying between $(V-I) = \sim 2$ mag and ∼3 mag could be PMS objects. In this CMD, to maintain clarity we have not plotted star No. 1548 despite it being detected in the I band, because it has $V-I$ colour of more than 6 mag. Star No. 449 may be a possible PMS

Table 3. The proper motion, parallax, and photometry by Gaia. The last column refers to likely or possible membership for each variable star.

ID	RA (degree)	DEC (degree)	μ_{ra} (mas/yr)	μ_{Dec} (mas/yr)	plx (mas)	gmag (mag)	bpmag mag	rpmag	mem
103	295.667936	23.412217	-1.392 ± 0.046	-5.264 ± 0.077	0.500 ± 0.074	17.288 ± 0.003	18.560 ± 0.015	16.172 ± 0.006	2
135	295.729818	23.406842	-1.335 ± 0.050	-5.330 ± 0.079	0.605 ± 0.085	17.340 ± 0.007	18.463 ± 0.025	16.006 ± 0.017	1
142	295.921757	23.403326	-4.224 ± 0.059	-6.330 ± 0.096	-0.125 ± 0.102	16.699 ± 0.003	21.455 ± 0.111	14.950 ± 0.005	0
147	295.717480	23.404825	-1.601 ± 0.043	-5.533 ± 0.068	0.154 ± 0.071	17.151 ± 0.003	18.555 ± 0.013	15.988 ± 0.005	1
154	295.729082	23.404078	-1.583 ± 0.012	-5.173 ± 0.018	0.411 ± 0.019	13.680 ± 0.003	15.006 ± 0.006	12.486 ± 0.006	2
177	295.798833	23.398720	-1.430 ± 0.059	-5.249 ± 0.097	0.382 ± 0.099	17.841 ± 0.003	19.238 ± 0.024	16.679 ± 0.007	2
201	295.806239	23.392781	-1.829 ± 0.065	-4.434 ± 0.111	0.764 ± 0.121	18.017 ± 0.003	18.879 ± 0.021	17.098 ± 0.009	1
213	295.678068	23.391730	-2.955 ± 0.072	-2.616 ± 0.122	0.692 ± 0.126	18.086 ± 0.003	18.923 ± 0.017	17.191 ± 0.008	0
238	295.856620	23.385850	-1.810 ± 0.048	-5.933 ± 0.080	-0.041 ± 0.079	15.379 ± 0.005	21.173 ± 0.091	13.658 ± 0.008	1
239	295.792933	23.386486	-1.545 ± 0.133	-5.335 ± 0.205	0.314 ± 0.186	19.537 ± 0.012	20.487 ± 0.072	18.373 ± 0.046	1
240	295.913449	23.384987	-2.683 ± 0.022	-9.082 ± 0.035	0.809 ± 0.037	16.070 ± 0.003	16.629 ± 0.004	15.346 ± 0.004	0
264	295.758973	23.382855	-1.839 ± 0.081	-4.993 ± 0.141	0.316 ± 0.146	18.200 ± 0.003	19.690 ± 0.028	17.004 ± 0.007	1
298	295.707379	23.376514	-1.757 ± 0.036	-4.931 ± 0.055	0.518 ± 0.058	16.844 ± 0.005	17.817 ± 0.017	15.833 ± 0.012	2
369	295.889138	23.363276	-2.759 ± 0.058	-5.104 ± 0.097	0.180 ± 0.097	17.647 ± 0.003	19.962 ± 0.039	16.257 ± 0.008	0
377	295.880082	23.361511	-1.767 ± 0.066	-5.422 ± 0.102	0.503 ± 0.107	18.157 ± 0.007	19.323 ± 0.030	17.036 ± 0.021	2
385	295.847545	23.360887	-1.713 ± 0.025	-4.949 ± 0.039	0.454 ± 0.041	16.211 ± 0.006	17.138 ± 0.021	15.246 ± 0.015	2
402	295.716202	23.358795	1.039 ± 0.544	-9.595 ± 0.908	-1.529 ± 1.016	19.114 ± 0.006	20.359 ± 0.063	17.606 ± 0.020	0
449	295.874874	23.347861	-1.534 ± 0.011	-5.289 ± 0.018	0.421 ± 0.019	14.456 ± 0.003	15.283 ± 0.003	13.559 ± 0.004	2
452	295.919127	23.346023	-1.632 ± 0.091	-5.204 ± 0.163	0.187 ± 0.154	18.342 ± 0.003	19.687 ± 0.034	16.889 ± 0.010	1
478	295.846924	23.343243	-2.242 ± 0.123	-5.663 ± 0.287	0.414 ± 0.207	18.715 ± 0.003	20.513 ± 0.146	17.239 ± 0.011	2
478	295.847334	23.343217	-1.835 ± 0.094	-5.443 ± 0.160	0.513 ± 0.166	18.445 ± 0.005	19.556 ± 0.035	16.804 ± 0.017	2
502	295.883889	23.339095	-1.539 ± 0.061	-5.143 ± 0.098	0.633 ± 0.100	17.859 ± 0.005	19.066 ± 0.032	16.755 ± 0.015	1
510	295.795529	23.339088	-1.736 ± 0.010	-5.177 ± 0.015	0.483 ± 0.016	13.870 ± 0.003	14.370 ± 0.003	13.188 ± 0.004	2
527	295.868122	23.335831	-1.350 ± 0.032	-5.299 ± 0.052	0.467 ± 0.055	16.580 ± 0.003	17.741 ± 0.006	15.496 ± 0.005	2
529	295.910436	23.335234	-1.692 ± 0.169	-5.130 ± 0.251	0.688 ± 0.245	19.127 ± 0.007	20.413 ± 0.056	17.532 ± 0.019	1
531	295.850017	23.335616	-1.798 ± 0.030	-5.427 ± 0.046	0.477 ± 0.050	16.447 ± 0.004	17.610 ± 0.013	15.360 ± 0.009	2
546	295.746235	23.334619	1.642 ± 0.054	-0.744 ± 0.078	0.666 ± 0.079	17.331 ± 0.003	18.235 ± 0.008	16.373 ± 0.004	0
561	295.717802	23.332530	-1.806 ± 0.058	-5.112 ± 0.077	0.449 ± 0.084	17.330 ± 0.003	18.517 ± 0.015	16.256 ± 0.006	2
576	295.862641	23.329178	-1.923 ± 0.092	-5.421 ± 0.138	0.003 ± 0.150	18.117 ± 0.004	19.508 ± 0.028	16.934 ± 0.008	1
614	295.686941	23.325122	0.064 ± 0.021	-2.606 ± 0.028	0.631 ± 0.030	15.454 ± 0.003	16.096 ± 0.004	14.665 ± 0.004	0
619	295.856809	23.323021	-1.705 ± 0.018	-5.254 ± 0.028	0.468 ± 0.030	15.271 ± 0.003	16.180 ± 0.004	14.321 ± 0.004	2
623	295.834392	23.322264	-5.268 ± 0.009	-19.204 ± 0.013	1.568 ± 0.014	12.832 ± 0.003	13.444 ± 0.003	12.086 ± 0.004	0
655	295.837455	23.317270	-1.973 ± 0.042	-5.777 ± 0.068	1.110 ± 0.079	16.811 ± 0.008	18.136 ± 0.032	15.636 ± 0.023	1
679	295.768320	23.313487	-1.905 ± 0.009	-5.483 ± 0.013	0.465 ± 0.015	13.468 ± 0.003	13.893 ± 0.003	12.833 ± 0.004	2
706	295.752612	23.310267	-1.994 ± 0.035	-5.380 ± 0.051	0.518 ± 0.052	16.539 ± 0.003	17.599 ± 0.007	15.508 ± 0.005	2
731	295.789104	23.307583	-1.690 ± 0.068	-5.348 ± 0.086	0.444 ± 0.094	17.553 ± 0.003	18.975 ± 0.020	16.406 ± 0.007	2
733	295.798253	23.307303	-1.671 ± 0.016	-5.453 ± 0.021	0.447 ± 0.022	14.822 ± 0.003	15.418 ± 0.003	14.057 ± 0.004	2
752	295.737297	23.306309	-4.190 ± 0.024	-9.756 ± 0.033	0.807 ± 0.036	15.715 ± 0.004	16.429 ± 0.010	14.875 ± 0.009	0
753	295.798228	23.305611	-1.439 ± 0.091	-5.723 ± 0.130	0.527 ± 0.132	18.213 ± 0.010	19.645 ± 0.052	16.983 ± 0.037	2
757	295.803663	23.305216	-1.823 ± 0.027	-5.343 ± 0.036	0.420 ± 0.038	16.075 ± 0.003	17.227 ± 0.006	15.000 ± 0.006	2
765	295.785197	23.304768	-1.971 ± 0.055	-5.559 ± 0.075	0.582 ± 0.084	17.403 ± 0.003	18.407 ± 0.020	16.391 ± 0.007	1
822	295.787697	23.296925	-1.931 ± 0.012	-5.372 ± 0.017	0.440 ± 0.020	14.172 ± 0.003	14.769 ± 0.004	13.413 ± 0.004	2
826	295.825083	23.296002	0.000 ± 0.000	0.000 ± 0.000	0.000 ± 0.000	18.717 ± 0.006	19.528 ± 0.088	16.822 ± 0.010	0
831	295.746221	23.296549	-3.198 ± 0.140	-6.012 ± 0.190	0.051 ± 0.164	18.030 ± 0.034	20.951 ± 0.092	16.343 ± 0.113	0
860	295.798251	23.292496	-1.763 ± 0.053	-5.198 ± 0.075	0.296 ± 0.086	17.181 ± 0.003	18.444 ± 0.012	16.091 ± 0.007	1
886	295.793856	23.290165	-1.700 ± 0.016	-5.457 ± 0.017	0.501 ± 0.019	14.140 ± 0.003	14.596 ± 0.003	13.490 ± 0.004	2
903	295.800965	23.287961	-1.443 ± 0.018	-5.239 ± 0.025	0.444 ± 0.025	14.092 ± 0.003	14.566 ± 0.003	13.425 ± 0.004	2
924	295.787347	23.285362	-1.173 ± 0.096	-7.786 ± 0.132	-0.663 ± 0.160	17.259 ± 0.004	18.378 ± 0.013	16.050 ± 0.006	0
945	295.855106	23.282160	-1.481 ± 0.027	-5.241 ± 0.040	0.579 ± 0.039	14.176 ± 0.003	14.745 ± 0.003	13.423 ± 0.004	1
950	295.706797	23.283426	-3.581 ± 0.166	-4.734 ± 0.244	1.034 ± 0.261	18.148 ± 0.004	21.250 ± 0.095	16.437 ± 0.008	0
951	295.796964	23.282188	-1.581 ± 0.030	-5.247 ± 0.043	0.424 ± 0.049	16.307 ± 0.003	17.417 ± 0.006	15.267 ± 0.005	2
965	295.891582	23.279985	0.251 ± 0.066	-2.097 ± 0.096	1.647 ± 0.102	14.281 ± 0.003	14.802 ± 0.004	13.562 ± 0.005	0
979	295.775108	23.280240	-1.692 ± 0.116	-5.685 ± 0.169	0.939 ± 0.173	18.478 ± 0.004	19.642 ± 0.032	17.336 ± 0.011	1
1000	295.814485	23.277802	-1.142 ± 0.009	-3.501 ± 0.013	0.635 ± 0.014	13.457 ± 0.003	13.714 ± 0.003	13.041 ± 0.004	0
1007	295.778155	23.276998	-1.989 ± 0.014	-5.533 ± 0.017	0.462 ± 0.020	14.277 ± 0.003	14.835 ± 0.004	13.530 ± 0.004	2
1025	295.690388	23.275981	-1.408 ± 0.245	-4.138 ± 0.340	0.725 ± 0.434	19.836 ± 0.011	20.939 ± 0.089	18.552 ± 0.043	0
1061	295.788730	23.269975	-1.671 ± 0.053	-5.426 ± 0.070	0.567 ± 0.076	17.298 ± 0.003	18.639 ± 0.013	16.154 ± 0.005	1
1063	295.778243	23.269561	-2.431 ± 0.095	-5.395 ± 0.081	0.282 ± 0.090	12.869 ± 0.003	00.000 ± 0.000	00.000 ± 0.000	1
1063	295.778279	23.270083	-1.210 ± 0.090	-5.981 ± 0.149	-0.091 ± 0.141	09.720 ± 0.003	09.906 ± 0.003	09.274 ± 0.004	1
1064	295.758524	23.270269	-2.317 ± 0.038	-4.554 ± 0.053	0.521 ± 0.058	14.183 ± 0.003	14.645 ± 0.003	13.493 ± 0.004	2
1066	295.843490	23.269270	-3.124 ± 0.021	-4.962 ± 0.028	0.291 ± 0.030	14.584 ± 0.003	16.863 ± 0.004	13.214 ± 0.004	0
1072	295.820520	23.269079	-1.645 ± 0.013	-5.282 ± 0.018	0.468 ± 0.019	14.395 ± 0.003	14.918 ± 0.003	13.690 ± 0.004	2
1087	295.798607	23.266730	-3.210 ± 0.068	-5.424 ± 0.095	-0.081 ± 0.102	16.758 ± 0.005	22.007 ± 0.122	14.938 ± 0.008	0

Table 3 – *continued*

ID	RA (degree)	DEC (degree)	μ_{ra} (mas/yr)	μ_{Dec} (mas/yr)	plx (mas)	gmag (mag)	bpmag mag	rpmag	mem
1094	295.817575	23.265043	−1.438 ± 0.023	−5.392 ± 0.032	0.428 ± 0.033	15.783 ± 0.003	16.830 ± 0.005	14.765 ± 0.005	2
1122	295.709131	23.260843	−1.586 ± 0.010	−5.419 ± 0.015	0.523 ± 0.017	13.588 ± 0.003	13.956 ± 0.003	13.029 ± 0.004	2
1151	295.805720	23.255733	−1.697 ± 0.114	−5.153 ± 0.163	0.173 ± 0.158	18.349 ± 0.007	19.909 ± 0.042	17.113 ± 0.021	1
1155	295.768235	23.255355	−1.672 ± 0.060	−5.173 ± 0.080	0.266 ± 0.087	17.543 ± 0.003	18.600 ± 0.015	16.523 ± 0.007	1
1168	295.883351	23.252588	−1.697 ± 0.098	−5.681 ± 0.144	0.519 ± 0.147	18.327 ± 0.004	19.726 ± 0.041	17.177 ± 0.010	2
1191	295.875000	23.248688	−1.715 ± 0.119	−5.193 ± 0.172	0.321 ± 0.183	18.703 ± 0.006	20.107 ± 0.041	17.449 ± 0.014	1
1228	295.850980	23.243847	−1.660 ± 0.116	−5.465 ± 0.169	0.200 ± 0.170	18.582 ± 0.005	20.077 ± 0.048	17.393 ± 0.013	1
1230	295.755855	23.244602	−1.353 ± 0.018	−5.260 ± 0.023	0.524 ± 0.025	14.356 ± 0.003	14.761 ± 0.003	13.759 ± 0.004	2
1235	295.672376	23.244490	4.176 ± 0.009	−1.613 ± 0.012	0.757 ± 0.013	12.759 ± 0.003	13.223 ± 0.003	12.126 ± 0.004	0
1262	295.774562	23.237761	−1.522 ± 0.228	−5.636 ± 0.521	0.437 ± 0.441	19.291 ± 0.006	00.000 ± 0.000	00.000 ± 0.000	2
1262	295.774980	23.237889	−0.719 ± 0.097	−4.431 ± 0.131	−1.092 ± 0.153	16.379 ± 0.003	17.455 ± 0.006	15.228 ± 0.007	0
1266	295.802542	23.236774	−1.624 ± 0.068	−5.081 ± 0.086	0.554 ± 0.093	17.741 ± 0.003	18.960 ± 0.022	16.686 ± 0.006	1
1268	295.698738	23.237776	−2.864 ± 0.083	−5.120 ± 0.113	0.230 ± 0.119	15.750 ± 0.004	21.208 ± 0.109	13.997 ± 0.007	0
1295	295.812280	23.232347	−1.564 ± 0.182	−4.156 ± 0.212	0.354 ± 0.225	18.726 ± 0.015	20.052 ± 0.046	17.061 ± 0.037	1
1298	295.671363	23.233613	−1.763 ± 0.227	−10.821 ± 0.301	−1.850 ± 0.289	18.089 ± 0.021	18.880 ± 0.071	16.384 ± 0.040	0
1317	295.899959	23.227779	−1.562 ± 0.101	−5.431 ± 0.123	0.589 ± 0.137	18.039 ± 0.010	19.288 ± 0.036	16.868 ± 0.028	1
1352	295.816693	23.222874	−0.419 ± 0.008	−4.078 ± 0.011	1.831 ± 0.012	12.449 ± 0.003	12.760 ± 0.003	11.975 ± 0.004	0
1389	295.717974	23.217819	−2.076 ± 0.024	−5.544 ± 0.032	0.434 ± 0.035	15.834 ± 0.004	16.701 ± 0.010	14.881 ± 0.008	2
1405	295.778615	23.214104	−0.016 ± 0.083	−4.330 ± 0.113	0.999 ± 0.120	18.085 ± 0.003	19.069 ± 0.014	17.103 ± 0.007	0
1406	295.844691	23.213100	−3.267 ± 0.064	1.679 ± 0.081	0.991 ± 0.089	17.530 ± 0.003	18.310 ± 0.023	16.559 ± 0.011	0
1459	295.758607	23.204733	−1.710 ± 0.090	−5.469 ± 0.124	0.343 ± 0.133	18.147 ± 0.003	19.354 ± 0.022	17.032 ± 0.008	1
1500	295.892106	23.195945	3.974 ± 0.049	−3.001 ± 0.071	0.924 ± 0.071	15.646 ± 0.003	16.328 ± 0.003	14.820 ± 0.004	0
1506	295.737755	23.197158	−1.684 ± 0.022	−4.291 ± 0.026	0.674 ± 0.028	15.219 ± 0.003	15.857 ± 0.004	14.435 ± 0.004	0
1508	295.846040	23.195095	−2.071 ± 0.089	−4.858 ± 0.124	0.392 ± 0.142	18.061 ± 0.005	19.437 ± 0.035	16.831 ± 0.013	2
1511	295.813526	23.194842	4.169 ± 0.025	20.500 ± 0.032	3.135 ± 0.035	15.890 ± 0.003	16.829 ± 0.004	14.933 ± 0.004	0
1525	295.817542	23.191915	−0.781 ± 0.009	−7.011 ± 0.012	0.655 ± 0.013	13.206 ± 0.003	13.785 ± 0.003	12.468 ± 0.004	0
1526	295.740382	23.192673	59.603 ± 0.010	−58.093 ± 0.014	9.066 ± 0.015	08.663 ± 0.003	08.977 ± 0.003	08.173 ± 0.004	0
1548	295.840568	23.186899	−1.083 ± 0.043	−3.305 ± 0.056	0.248 ± 0.060	13.737 ± 0.003	18.375 ± 0.013	12.116 ± 0.006	0

star, but its placement in the $U - B/B - V$ and $J - H/H - K$ TCDs suggests a field star, even though it has proper motions in the range of probable cluster members.

3.2.6 NIR CMDs

The J versus $(J - K)$ and J versus $J - H$ CMDs for the present sample of variable stars are shown in Fig. 16. it is seen that the MS is almost vertical and clearly separated from the PMS objects/field stars as in the case of the V versus $(V - I)$ CMD. Bica et al. (2008) described the same and from statistical cleaned CMD, they found that two populations are distributed separately where majority of PMS objects are faint and redder. They found the age of the cluster in the range from 2 to 7 Myr, a colour excess of $E(B - V) = \sim$0.86 mag, and $A_V = 2.7 \pm 0.2$. In their work after fitting theoretical models, the absolute distance modulus of the cluster was found to be $(m - M)_O = 11.5$ mag.

Although stars numbered Nos. 142, 402 826, 950, 924, 1025, 1066, 1087, 1298, and 1548 are nonmembers from the analysis of the Gaia data, we have considered them as possible PMS objects based on their positions in different CMD and TCDs. We note that there are 10 stars, namely, Nos. 240, 614, 623, 752, 965, 1235, 1352, 1500, 1525, and 1526, that are designated as nonmembers from proper motion and parallax and, these could be MS stars based on location in TCDs and CMDs. Star 1506 is located well away from the MS in $U - B/B - V$ TCD, while it is lying on the MS in $V/V - I$, $J/H - K$, and $J/J - H$. The analysis of Gaia data also found it to be nonmember. This is a doubtful case for being an MS member. From Gaia data analysis, we found stars Nos. 201, 239, 449, 619, 765, 861, 1151, 1168, 1191 and 1508 as possible or probable members, but their locations in various TCDs and CMDs do not seem to be consistent with membership. Thus, these are considered field stars.

We looked for the matches of our eight previously identified PMS stars based on their 2MASS colors and their spectra taken at the 2.16 m telescope of Beijing Observatory (Hojaev et al. 2003). The spectra showed the strong H-alpha in emission, the SED in continuum, and other features typical either for TTS or Herbig Ae/Be stars. The cross-match yields three common stars, namely 154, 655, and 679; for two of them, we have already determined their features (their location on the diagrams, their proper motions, and parallaxes). In the present work, we have classified 655 as classical TTS and 679 as MS. There was doubt to consider 679 as PMS because in $U - B$ versus $B - V$ TCD it is lying on MS, but in $J - H$ versus $H - K$ diagram it is placed in the location of classical TTS. Now, we determined the membership of star No 154. It might be a probable member of the cluster as Herbig Ae/Be type star, while earlier (Hojaev et al. 2003) it has been classified as classical TTS; though it has very different position in V versus $V - I$ CMD to be PMS star, GAIA suggests it to be a highly probable member, and in $J - H$ versus $H - K$ it is located where Herbig Ae/Be stars are found. Therefore, it could be considered as Herbig Ae/Be star.

We have considered members those stars that fulfil criteria like location in TCDs, CMDs, and have consistent kinematics. Therefore, using proper motion data together with location in various TCDs and CMDs obtained from present and available photometric *UBVI*, *NIR*, and *MIR* data, we classify 25, 48, and 15, respectively, as MS, PMS members of the cluster, and field stars. The classification of variables is given in Table 4.

Table 4. Period and amplitude of variable stars. Last column represents membership classification of stars along with their classification based on variability characteristics. The stars with asterisk are previously known variables. The cTTS, wTTS, and HAe/Be are classical, weak-lined TTS, and Herbig Ae/Be star, respectively.

ID	Period (days)	Period (TESS) (days)	Amp. (mag)	class.
103	1.919	1.913	0.087	PMS, wTTS
135	0.041, 0.010	–	0.336	PMS, cTTS
142	0.504	–	0.156	PMS, wTTS
147	0.940, 0.071	–	0.080	PMS, wTTS
154	1.008	–	0.580	PMS, HAe/Be
177	0.784	–	0.129	PMS, wTTS
201	0.850, 0.845	–	0.115	Field
213	0.253, 0.509	–	0.167	Field
238	0.497	–	0.166	Field
239	0.506, 0.969	0.889, 2.429	1.028	PMS, wTTS
240	1.109, 0.067	2.253	0.032	MS
264	0.546	–	0.202	PMS, wTTS
298	0.357, 0.082	–	0.107	PMS, HAe/Be
369	5.699	2.400, 0.600, 7.041	0.288	PMS
377	0.0332	–	0.103	Field
385	30.100, 0.958	5.243, 3.960, 0.939	0.425	PMS, HAe/Be
402	0.804	–	0.394	PMS, wTTS
449	3.852, 0.789	5.297, 0.713, 4.084	0.037	Field
452	3.572	–	0.203	PMS, wTTS
478	9.199, 0.898	3.066, 2.622, 0.902	0.366	PMS, wTTS
502	1.138, 0.887	–	0.238	PMS, wTTS
510	0.143, 0.030	–	0.025	MS, New
527	0.671, 2.057	2.045, 2.879	0.168	PMS, wTTS
529	0.047	–	0.290	PMS, wTTS
531	0.755, 3.064	3.084, 6.232, 9.713	0.219	PMS, wTTS
546	0.806, 0.057	–	0.044	Field
561	10.300, 0.909	3.24	0.149	PMS, wTTS
576	0.882	0.850, 3.715	0.237	PMS, wTTS
614	0.707	0.705, 1.775	0.051	MS
619	0.852	3.825, 0.850	0.030	Field
623*	0.044, 0.053	0.153, 1.595	0.022	MS
655*	17.716, 0.030	–	0.236	PMS, cTTS
679	1.1242, 0.059, 0.564	0.565, 3.376	0.046	MS
706	4.336, 0.561	–	0.049	PMS, wTTS
731	0.359, 0.099	–	0.065	PMS, wTTS
733*	0.512, 0.143	–	0.029	MS
752	0.153	0.153, 10.770	0.257	MS
753*	0.036	–	0.225	PMS, cTTS
757*	0.553	–	0.125	PMS, wTTS
765	0.112, 0.124	–	0.133	Field
822*	0.143, 0.084	–	0.034	MS, New
826	0.072	–	0.139	PMS, wTTS
831*	1.009	1.147, 1.545, 1.095	1.463	Field
860	8.517, 0.523	–	0.197	PMS, cTTS
886*	0.446, 0.618	–	0.032	MS
903*	0.848	–	0.033	MS
924*	3.206, 0.59, 0.759	–	0.123	PMS, wTTS
945	0.662, 0.663, 1.965	1.966, 6.000	0.026	MS
950	0.504	3.179, 2.442	0.265	PMS, wTTS
951	1.392, 0.775	–	0.064	PMS, wTTS
965	2.661, 0.726	2.65, 4.805	0.053	MS, New
979*	0.036	0.064, 5.002	0.185	PMS, cTTS
1000	0.042, 0.486	–	0.016	MS, New
1007*	0.064	0.527, 0.064, 4.818	0.037	MS
1025	0.059	–	0.600	PMS, wTTS
1061*	0.438	1.581, 6.269	0.099	Field
1063	1.049, 0.028	–	0.131	MS, β Cep
1064	0.653, 0.059, 0.395	0.804, 5.291	0.025	MS
1066	0.0518, 0.082	2.166, 1.203	0.013	PMS, wTTS
1072	0.484, 0.032	0.819, 11.649	0.025	MS New
1087*	0.125	–	0.103	PMS, wTTS
1094	0.815	–	0.081	PMS, wTTS
1122	2.402, 0.705	0.705, 11.649	0.039	MS, SPB
1151	0.769	0.153, 4.834	0.359	Field
1155	10.955, 0.100	–	0.092	PMS, wTTS
1168	0.526	–	0.240	Field
1191	0.924	–	0.481	Field
1228	0.902	–	0.448	PMS, wTTS
1230	0.386, 0.629	0.385, 1.755	0.019	MS, New
1235	1.622, 3.267	3.243	0.211	MS, New
1262	1.215, 0.446	–	0.058	PMS, wTTS
1266	3.382	–	0.148	PMS, wTTS
1268	63.269	5.240, 0.996	0.276	PMS, wTTS
1295	0.028	–	0.495	PMS, cTTS
1298	0.983, 0.496	–	0.438	PMS, cTTS
1317	0.485	–	0.671	PMS, cTTS
1352	0.027, 0.336	–	0.014	MS, SBP
1389	0.111, 0.166	–	0.086	PMS, HAe/Be
1405	0.077, 0.064	–	0.128	Field
1406	0.140, 0.082	–	0.123	Field
1459	0.865	–	0.172	PMS, wTTS
1500	0.072	–	0.046	MS
1506	0.259, 0.491	–	0.031	MS
1508	0.027	–	0.264	Field
1511	0.059, 0.110	–	0.032	Field
1525	1.132, 0.063	–	0.034	MS, New
1526	0.058	–	0.075	MS
1548	0.986, 0.329	–	0.174	PMS, wTTS

4 CHARACTERISTICS OF VARIABLE STARS

The log $(L/L_{\odot})$ vs log $T_{\rm eff}$ diagram ($H-R$ diagram) for 21 members (MS variables) is shown as in Fig. 17. We are not able to locate four MS star Nos. 240, 752, 1107, and 1500 in this plot due to lack of their U and B band data. Here, the effective temperature and bolometric correction (BC) have been determined from Torres relation (2010) using the intrinsic $(B-V)$ colour. The $M_{\rm bol}$ values of stars are obtained from the relation $M_{\rm bol} = M_V + BC$, where M_V is the absolute V-band magnitude. The luminosity was obtained from the relation $\log(L/L_{\odot}) = -0.4(M_{\rm bol} - M_{\rm bol_{\odot}})$, where $M_{\rm bol_{\odot}}$ is the bolometric magnitude for the Sun. The MS variable stars have been classified according to their periods of variability, the shape of light curves, and their positions in the H-R diagram. We detected one star as β Cep-type. Four star Nos. 679, 886, 1122. and 1352 are located in the instability strip of SPB stars. The positions in the cluster H-R diagram as well as the observed variability characteristics of nine stars allow us to conclude that these variables belong to the new class variables. One star based on its location in the $H-R$ diagram should be δ Scuti-type variable.

In the present study, we have detected 48 PMS stars as most likely cluster members in the PMS stage of evolution. Of these, 4, 8, and 36 stars are classified as Herbig Ae/Be stars, classical TTSs, and weak-lined TTSs, respectively. The amplitudes of weak-lined TTSs range from ∼0.05 to ∼0.2 mag, and most weak-lined TTSs vary with

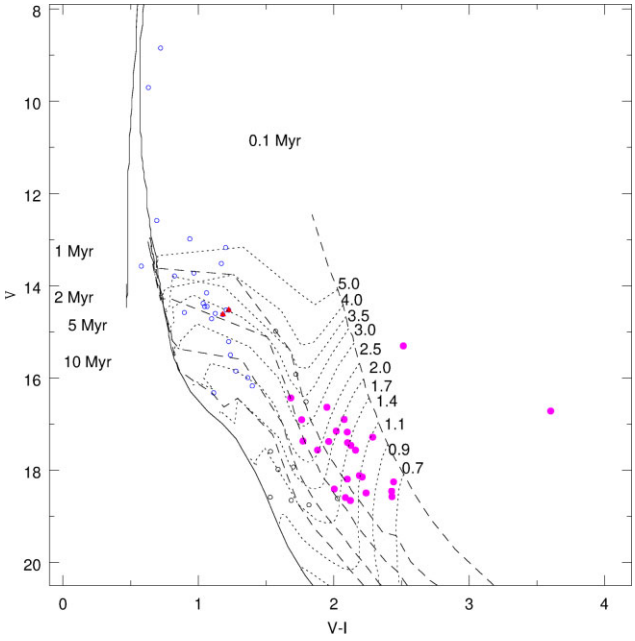

Figure 15. $V/(V-I)$ CMD for variable stars in the region of the cluster NGC 6823. The open circles (blue) are MS variables, and probable PMS variable stars are shown by filled circles (magenta). The open circles in black colour are considered field stars. The continuous curve is ZAMS by Girardi et al. (2002) while dashed lines are PMS isochrones taken for 0.1, 1, 2, 5, and 10 Myrs (Siess et al. 2000). The PMS evolutionary tracks for different masses ranging from 0.7 to 5.0 $M_{\odot}$ from Siess et al. (2000) are plotted with dotted curves. BL 50 and HP 57 are shown by red triangles.

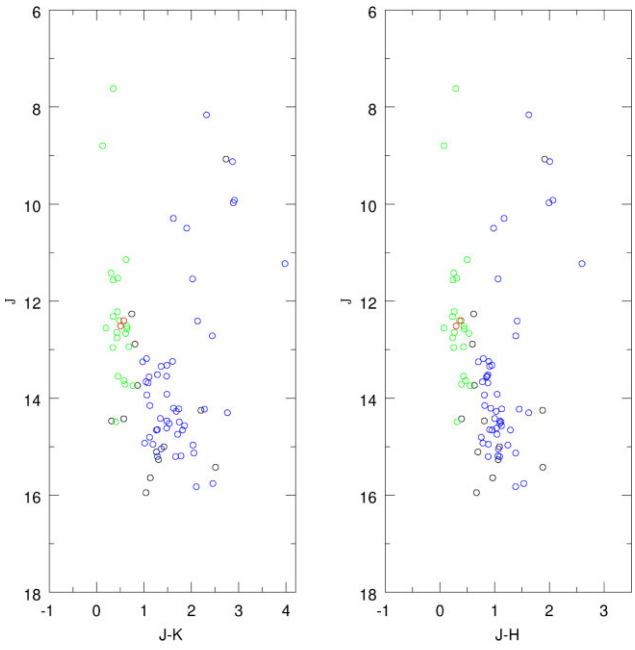

Figure 16. $J/(H-K)$ and $J/(J-H)$ CMD for variable stars detected in the field of NGC 6823. The *JHK* data have been taken from the 2MASS catalogue (Cutri et al. 2003). Circles (blue) and circles (green) represent MS and PMS, respectively. The Open circles in black colour demonstrate the field stars. The locations of star Nos. 822 (BL 50) and 1007 (HP 57) are shown with an open circle in red colour.

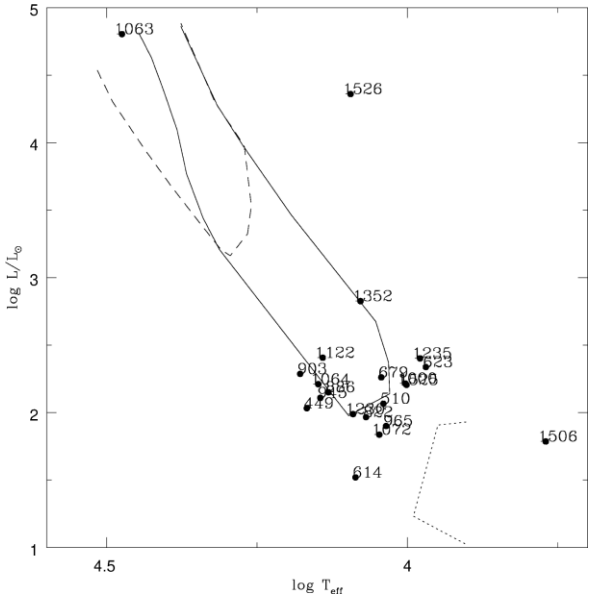

Figure 17. $\log(L/L_{\odot})/\log T_{\rm eff}$ diagram for the probable MS variable stars identified in the present study. The continuous curve represents the instability strip of SPB stars, whereas dotted curve shows the instability region of δ Scuti stars. The dashed curve shows the location of β Cep stars (cf. Balona et al. 2011).

shorter periods of less than 1.0 days. The periods and amplitudes of classical TTSs are found to range from ∼0.05 to ∼30 days and ∼0.2 to ∼0.7 mag, respectively. The above results suggest that stars with discs, i.e. classical TTSs, exhibit relatively larger amplitudes than the weak-lined TTSs do, with the stellar variability in classical TTSs arising from the presence of the spots, hot and cold, on the stellar surfaces as found in the previous studies (e.g. Bouvier et al. 1993; Pandey et al. 2019).

4.1 Known variables

In the CCD search for variable stars in NGC 6823, Pigulski et al. (2000) demonstrated that all stars with spectral types later than A0 are PMS objects. They detected two variable stars of δ Scuti type and these stars could be at the PMS stage of evolution and suggested that these objects can further be used to test the evolutionary changes in this class of variable stars. The CMD was used to compare and discuss the position of the two discovered δ Scuti stars with reference to the theoretical instability strip for PMS stars of this type. They also have 13 other variables, including one bright cluster eclipsing binary and an SPB candidate.

Of the 15 variables identified by Pigulski et al. (2000), 14 were found to be variable in the present work. We could not detect variability in the star H8 (E88 or BL 4) (B0 V:pe by Turner 1979), B1.5 V by Massey et al. 1995), and B1 V by Shi & Hu (1999). Pigulski et al. (2000) noted this star as the brightest variable member in the observed cluster field and found it to be a binary star where only one eclipse was detected in the *I* band.

Now we will describe the nature of all the known 14 variable stars individually.

Stars BL 50 (822) and HP 57 (1007) with periods of 0.0718530 and 0.10114 days for BL 50, and 0.0785819 and 0.0644149 days for HP 57 were found to be most likely cluster PMS members by Pigulski et al. (2000). With their positions in the cluster CMD as well as the observed periods, Pigulski et al. (2000) concluded that both objects

could be δ Scuti variables. The present membership analysis, i.e. from kinematics and positions in various CMDs and TCDs, suggests both stars to be MS members. In the H-R diagram, star No. 822 is positioned where new class variables are found (between the red edge of SPB and the blue edge of δ Scuti instability strip). Star No. 1007 could not be placed in the H-R diagram due to unavailability of *UBV* data. The present period of stars 822 is derived as 0.143 days and 0.084 days, whereas the periodogram analysis gives period of 0.064 days for star 1007. The period derived for star 1007 is in good agreement with that derived by Pigulski et al. (2000). The location of these two stars were shown with red and black triangles in V versus $(V-I)$ CMD and $J-H$ versus $H-K$ TCD, respectively.

Star No. 903, a probable cluster MS member was discovered as the third pulsator (G 51) by Pigulski et al. (2000). Its brightness varies with a period of 0.848 days with an amplitude about 0.03 mag. The star was classified by Pigulski et al. (2000) as an SPB variable according to their variability characteristics.

The brightness of star No. 886 (G52) found to be binary by Pigulski et al. (2000) varies with period of 0.61 days with an amplitude 0.03 mag. It is diagnosed as a member of the cluster from proper motion and its location in various photometric diagrams. The present estimates for period and amplitude are consistent with those reported in Pigulski et al. (2000).

Star No. 733 has proper motion values of $\mu_\alpha = -1.671$ mas/yr and $\mu_\delta = -5.453$ mas/yr; hence, it is a probable member of the cluster. Our analysis suggests possibly more than one period, with 0.143 and 0.512 days. In Pigulski et al. (2000) it is H30, and they found its period of more than 3 days.

The brightness of star No. 757 was found to be changing with one single period of 0.553 days. The present work classified this star to be a probable PMS cluster member. Pigulski et al. (2000) named it V2 and derived its period of about 1.24 days, commenting that the true period for this star corresponds to an alias frequency, and they found this star to be of PMS-type source. The present observations confirm its variability and PMS nature. The light curves and periodogram analysis manifest that it could be an eclipsing binary with primary and secondary depths being nearly equal. Morales-Calderon et al. (2012) found six new candidate sources as PMS-eclipsing binaries with multi-epoch data of about 2400 stars associated with the Orion Nebula Cluster, and it is stated that the PMS-eclipsing binaries are valuable as they are in the stage of PMS evolution which is highly dynamic; therefore, their detection is rare at this stage.

Star No. 924 may be a PMS variable with a light curve varying with more than one period. The proper motion suggests a nonmember of the cluster, but its position in TCDs and CMDs indicates a possible weak-lined TTSs. It is designated as V4 by Pigulski et al. (2000).

Star V5 of Pigulski et al. (2000) is numbered as No. 1061 in this work. We considered it a field star based on its location in CMDs and TCDs. Its brightness in V and I bands varies with a period of 0.438 days. The variability of this star is confirmed in the present work.

Star V8 (979) which could be a classical TTS based on its location in the $J-H$ versus $H-K$ diagram. It has a period of about 0.038 days. The kinematic data indicate it to be a possible member of the cluster of PMS nature. Pigulski et al. (2000) also found it to be suspected PMS variable.

Star No. 753 was designated as V7 by Pigulski et al. (2000). The period of V7 could not be found by Pigulski et al. (2000) due to either irregular brightness or long-period variations. In our analysis, this star is considered a probable member of the cluster according to the proper motion study. Its position in the CMD and TCDs suggests a PMS Class II object. This star shows periodic brightness variation with its period and amplitude being 0.036 days and 0.225 mag, respectively.

Star No. 655 (V3 in Pigulski et al. 2000) is a periodic variable with two possible periods, of about 17 days and of 0.059 days. The location of this star in the $J-H$ versus $H-K$ TCD suggests a Class II source, while proper motion data also suggest cluster membership.

Star No. 1087 is found to be nonmember based on its proper motion values. Its location in TCDs suggests a PMS source. Its brightness changes periodically with a period of ∼0.125 days. In Pigulski et al. (2000) this star (V1) was the reddest object among their variable sample.

Star No. 831 is referred to as V6 by Pigulski et al. (2000) and they found this star too red as a member of the cluster. We confirm this star, with a period of about 1 day, to be a field star.

Star No. 623, E 100, is a PMS object, though it was considered as a nonmember of the cluster in Pigulski et al. (2000) because its proper motion values were different from those of cluster members (Erickson 1971). They mentioned that this star might belong to the foreground population and it is of a late-type object. The present estimation of its membership using Gaia data also finds it to be a nonmember.

4.2 Newly detected variables

Now we present newly identified variables in this work. Star No. 1235 is classified, on the basis of the shape of its light curve, to be an eclipsing binary, bearing similarity to that of an EA (Algol) type. In EA-type eclipsing binaries, both stars are nearly spherical in shape, with an extremely wide range of periods from 0.2 to 10 000 days, and with a wide range of amplitude of variability. Star No. 1235 has a period of 1.622 days and a variation amplitude of 0.211 mag. In the $H-R$ diagram, this star is found to be located in the region of new class variables. More observations of this star are required to confirm its nature. This star is a member of the cluster based on locations in TCDs. However, Gaia data suggest it to be a nonmember of the cluster.

The light curves of star No. 449 in both V and I bands reveal it to be a short-period variable. Its periodogram in both V and I exhibits peaks around 3.2 and 0.789 days. Gaia data suggest it to be a probable member.

The variability of the star No. 527 suggest that it is a periodic variable whose light varies with a period of 0.671 days. It is found to be a probable member of the cluster from its proper motion measurements. Its location in CMDs and TCDs indicates it to be a PMS object.

The brightness of star No. 531, a probable PMS member of the cluster, is found to vary with a period of 0.755 or 3.065 days, with the variability characteristics consistent with TTSs.

The proper motion values are not in favour of star No. 752 to be a cluster member, though in the V versus $V-I$ CMD, it is located along the MS. The period is derived as 0.153 days and the amplitude is about 0.2 mag. The variability characteristics of this star is similar to a pulsating type star or eclipsing binary. After doubling its period, its light curves show two minima that have almost equal depth. It could be an EW-type eclipsing (W Ursae Majoris eclipsing system). The EW-type variables have periods of less than 1 day, with almost equal depths of primary and secondary minima.

Star No. 1508 has a period of ∼0.027 day with an amplitude of about 0.2 mag. This variable resembles that of the SX Phe type (Cohen & Sarajedini 2012), which are similar to δ Scuti stars but pulsate with amplitudes up to 0.7 mag according to the variability types listed in the General Catalogue of Variable Stars (GCVS).

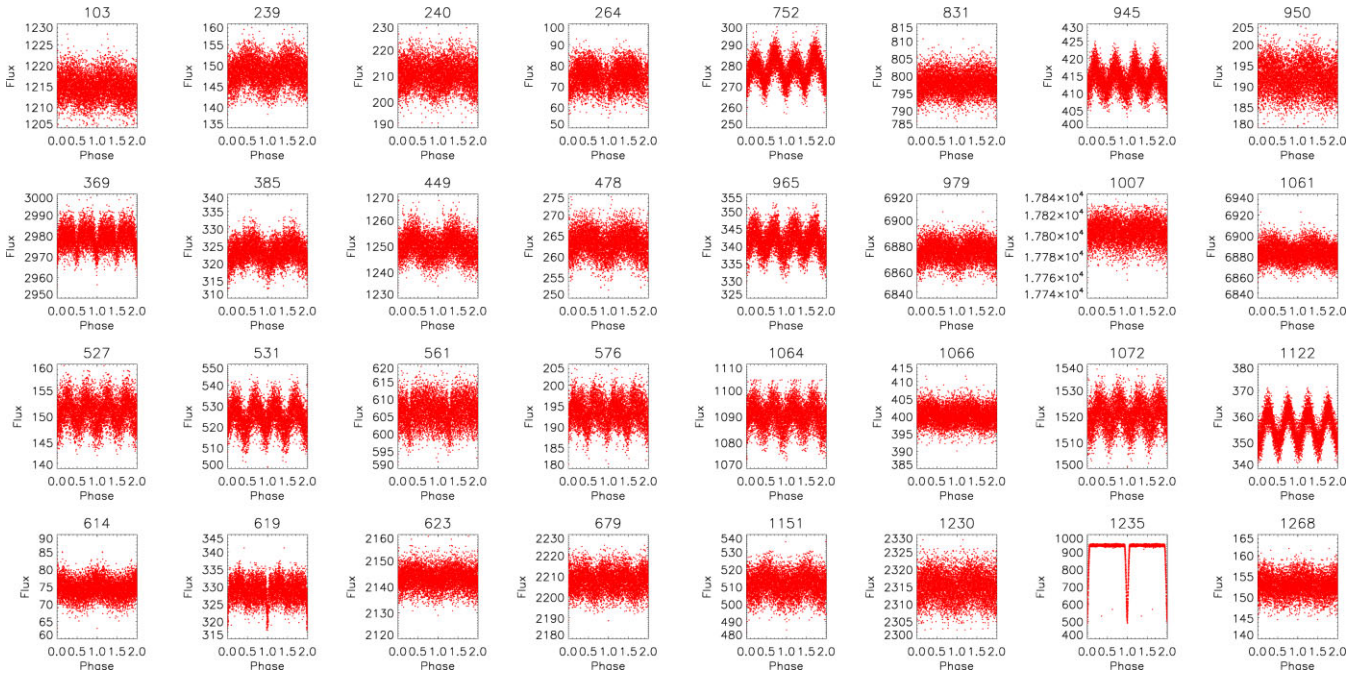

Figure 18. The phased light curves of variable stars using TESS data.

5 TESS LIGHT CURVES

A few variables like No. 1235 and No. 752 have times series data from the TESS (Ricker et al. 2015). The high-quality light curves from the TESS can be used to understand stellar and planetary evolution and these data provide us opportunity to study the rotation of stars (Canto Martins, Gomes & Messias 2020). Here, we present folded light curves, exhibited as Fig. 18 for 32 stars that do not have flux contribution from nearby brighter sources to account for the low spatial resolution of TESS. TESS observes the sky in sectors with each sector observed for about 27 days. The eleanor pipeline to extract times series data of objects from TESS images has been used, which is an open-source tool (Feinstein, Montet & Foreman-Mackey 2019, https://archive.stsci.edu/hlsp/eleanor). We can use the eleanor package to create light curves for fainter objects for a more detailed or optimized analysis of individual objects (Feinstein et al. 2019). The eleanor uses TESS Full Frame Images (FFIs) to extract systematics-corrected flux for any given star observed by TESS. It takes TIC ID, coordinates (RA and DEC) of a star. First, the raw flux is calculated by aperture photometry as RAW_FLUX that is background subtracted. This raw flux is then corrected for possible systematic effects, which creates a flux called CORR_FLUX. For isolated stars, to obtain the corrected flux we have taken default apertures. The eleanor software also provides the option to define one's own aperture. We have extracted light curves of all the detected in the present photometry.

Out of 32 variables, there are 7 stars that are diagnosed as PMS and 14 as MS. The periods of all the 32 stars have been determined using the method described in the Section 2.1. The periods for 14 stars (103, 527, 531, 576, 614, 619, 679, 752, 945, 965, 1007, 1122, 1230 and 1235) are found to be in good agreement with that obtained from the present ground-based optical data. The nature of star No. 752 and No. 1235 as mentioned earlier is confirmed from their TESS light curves; that is, star No. 752 shows unequal maxima, likely due to the O'Connell effect (O'Connell 1951), for which the maxima between eclipses in some eclipsing binaries are not found equal in brightness (Knote et al. 2022). The phased light curves of star Nos. 369, 561, and 619 show brightness variations similar to Algol-type eclipsing binaries. The light curves of stars 527, 531, 576, 965, 1064, 1072, and 1122 were folded by doubling the value of their derived period. Three stars 527, 531, and 576 of them are probable PMS stars, while the remaining four stars are cluster members of MS type. The folded light curves and periods of 1064, 1072, and 1122 are similar to the variability characteristic of EW-type variables. The light curve of star 576 seems to have properties of EA-type variable. The stars 527 and 965 could be weak-lined TTSs based on their variability characteristics, as these sources are of PMS nature and show periodic variability. The period of star 531 was derived as 3.084 days using TESS data, while its period comes out to be 0.755 days from V and I band light curves. The variability characteristics for those stars whose periods determined from present V and I data do not match with that derived from TESS observations could be revisited in the future observations of the cluster NGC 6823. The conflicts between periods for some cases may arise due to the contribution of flux from nearby stars in TESS data despite being selected isolated stars. The present work identified five MS, four PMS stars, and one field variable of eclipsing nature, two of which are confirmed eclipsing binaries and remaining are suspected ones. Their derived parameters are listed in Table 5. The masses and ages of two suspected PMS binaries could not be obtained due to unavailability of their $V - I$ colour. Since *UBV* data of MS star no. 752 are not available, the temperature for this star has been obtained using theoretical models of Girardi et al. (2002) and present V magnitude.

6 CORRELATION BETWEEN CIRCUMSTELLAR DISCS AND VARIABILITY

Accretion onto the stellar surface creates hotspots that brighten the light curve up to 3 mag, whereas the magnetic field is responsible for cool and therefore dark spots. Herbst et al. (1994) studied photometric

Table 5. The derived parameters of the confirmed/suspected eclipsing binaries. The last column refers to binary classification.

ID	Age Myrs	Mass $M_\odot$	M_{bol} mag	log $(L/L_\odot)$	log T_{eff}	class.	Binary class.
369	–	–	–	–	–	PMS	EA?
561	1.3	1.28	–	–	–	PMS	EA?
576	–	–	–	–	–	PMS	EA?
619	–	–	–	–	–	Field	EA?
752	4.0	1.95	–		3.915	MS	EW
757	0.4	1.50	–	–	–	PMS	EW?
1064	4.0	3.40	− 0.794	2.211	4.148	MS	EW?
1072	4.0	3.20	0.1394	1.837	4.047	MS	EW?
1122	4.0	4.59	− 1.286	2.407	4.141	MS	EW?
1235	4.0	6.75	− 1.272	2.402	3.979	MS	EA

variability of PMS stars in the Orion Nebula Cluster and showed that slower rotators have larger IR excess than fast rotators, indicating disc-locking, for which the angular momentum is transported through magnetic field lines from the central star to the circumstellar disc. This supported the results by Edwards et al. (1993) for which low-mass young stars with accretion discs have periods more than 4 days, whereas stars without have periods ranging from 1.5 to 16 days. Rotation seems to be regulated after the disc is dissipated, as the star spins up while contracting towards the MS (Bouvier et al. 2007). These results support the magnetic-disc model, which controls PMS winds and angular momentum of young stellar objects during the PMS evolution.

Models for a disc–star interaction (Ghosh & Lamb 1979; Shu et al. 1994; Ostriker & Shu 1995) are supported by the rotation periods of PMS objects in young open star clusters (Attridge & Herbst 1992, Herbst, Bailer-Jones & Mundt 2001; Herbst et al. 2002, 2004). Kearns & Herbst (1998) and Nordhagen et al. (2006) determined the rotation periods in two clusters. James et al. (2010) derived light-curve periods of sun-like sources in the young cluster NGC 1039. Lamm et al. (2004) presented the rotation period of PMS objects, which supports the disc-locking mechanism in young stars. Broeg et al. (2006) measured rotational periods of young objects to understand the star-formation scenario that the off-cloud young sources should rotate faster if these objects were ejected from the cloud. They did not find significant period distribution off-cloud weak-lined TTS south of Taurus-Auriga with respect to weak-lined TTS inside the Taurus-Auriga molecular cloud. Godoy-Rivera, Pinsonneault & Rebull (2021) studied stellar rotation and found that the distribution of period with mass in the case of open clusters gives important constraints to study angular momentum evolution and it is evident that spin down process depends on the mass. The rotation periods of the members of cluster have been presented, which are found to be in range from 0.5 to 11.5 days (Meibom, Mathieu Robert & Stassun 2009, Meibom et al. 2011). Gondoin (2018) concluded that the stellar rotation evolution in open star clusters could be from loss of angular momentum, which occurs due to strong winds during the early evolution of young solar-type stars.

A disc-bearing YSO spins down due to magnetic braking (Koenigl 1991; Ostriker & Shu 1995). The increasing disc fraction with rotation period in open clusters was reported by Cieza & Baliber (2007). As discussed above, to explore a correlation between the variability of classical TTSs with colour excess, mass, and age, we have plotted amplitude of variability with $\Delta(I-K)$ excess in Fig. 19 (left panel), while the right panel of Fig. 19 shows the rotation period with $\Delta(I-K)$ excess. Here the $\Delta(I-K)$ excess of PMS sources is determined using the following relation,

$$\Delta(I-K) = (I-K)_{obs} - (A_I - A_K) - (I-K)_0,$$

where $(I-K)_{obs}$ and $(I-K)_0$ are the observed and intrinsic colours of stars, whereas A_I and A_K denote the interstellar extinction in the I and K bands, respectively. To estimate the value of $(I-K)_0$ of YSOs, it was necessary to estimate their masses and ages. These values are available for only 22 PMS objects from the V versus $V-I$ CMD after comparing with the theoretical models of Siess et al. (2000). Of the 22 sources, there are 4 classical TTSs for which we could estimate the age and mass. The A_I and A_K are estimated using the relations given by Cohen et al. (1981) by adopting $A_V = 2.24$ mag. The $(I-K)_0$ value is obtained from the PMS evolutionary models of Siess et al. (2000) of a given mass and age. Fig. 19 (left panel) shows that a larger $\Delta(I-K)$ value for classical TTSs corresponds to a relatively larger amplitude of variability, consistent with those found in the literature, though we find no clear correlation between $\Delta(I-K)$ and rotation period. However, one classical TTS No. 655 with larger $\Delta(I-K)$ excess is found to be rotating with a longer period.

7 SUMMARY

This work presents 88 variable stars in the young star cluster NGC 6823. The association of detected variables to the cluster has been discussed with the Gaia kinematic data, and the optical and NIR TCDs and CMDs. The membership of previously known variables has also been discussed. We have detected 48 stars as PMS stars, of which 8 are classified as classical TTSs, while 36 and 4 as weak-lined TTSs and Herbig Ae/Be stars, respectively. Three known variables H30, V2, and V8 are found to be PMS variables as suggested by Pigulski et al. (2000) while two stars BL 50 and HP 57 previously detected as PMS δ Scuti pulsators are turned out to be MS members of the cluster from their proper motion, parallax values, and positions on the TCDs and CMDs. TTSs have periods ranging from 0.01 days to 30 days, and amplitudes of brightness variation from 0.05 mag to 0.7 mag, with the classical TTSs varying generally with larger amplitudes than weak-lined TTSs do. It is noted that three of the four classical TTSs with larger values of the disc indicator ($\Delta(I-K)$) are found to have relatively larger amplitude variation. The present results do not support the disc-locking mechanism; however, one classical TTS having large $\Delta(I-K)$ is found to be rotating slowly. In addition, we have identified 25 stars to be MS variables (SPB stars, δ Scuti, β Cephei, and new class variable stars). Their variability has been characterized based on the period, amplitude, shape of the light

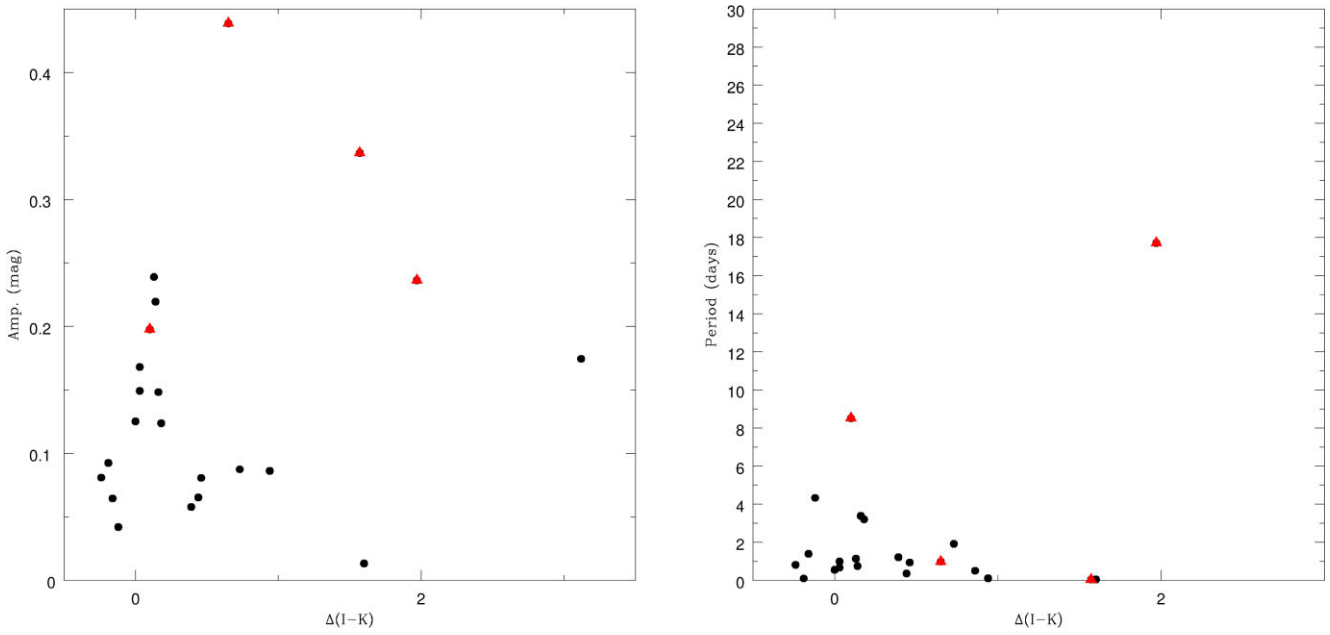

Figure 19. Amplitude of variability and rotation period of TTSs with $\Delta(I-K)$ is shown.

curves, and location on the $H-R$ diagram. Fifteen variable stars may belong to the field star population.

ACKNOWLEDGEMENTS

We are thankful to Prof. E. L. Martín for the valuable suggestions that improved scientific content of the present work. Late Dr. A. K. Pandey facilitated this collaboration project as Director of ARIES during WPC's visit. He will be forever remembered. SL will always be grateful to him for all the support and encouragement. We acknowledge the assistance of Michael Schwartz who managed the Tenagra Observatory in acquisition of the images of this study. ASH and JCP thanks Ministry of Innovation Development of Uzbekistan and Department of Science and Technology of India for financing the joint project (Project References: UZB-Ind-2021-99 & INT/UZBEK/P-19). This publication makes use of data products from the 2MASS, which is a joint project of the University of Massachusetts and the Infrared Processing and Analysis Center/California Institute of Technology, funded by the National Aeronautics and Space Administration and the National Science Foundation. This paper includes data collected by the TESS mission. Funding for the TESS mission is provided by the NASA's Science Mission Directorate. We also acknowledge 'Galactic Legacy Infrared Midplane Survey Extraordinaire' (GLIMPSE) Legacy Program for Spitzer IRAC data. This work also used data from the European Space Agency (ESA) space mission Gaia. Gaia data are being processed by the Gaia Data Processing and Analysis Consortium (DPAC). Funding for the DPAC is provided by national institutions, in particular, the institutions participating in the Gaia MultiLateral Agreement (MLA). The Gaia mission website is https://www.cosmos.esa.int/gaia. The Gaia archive website is https://archives.esac.esa.int/gaia.

DATA AVAILABILITY

The data underlying this article will be shared upon request to the corresponding author. The 2MASS data are available at https://vizier.u-strasbg.fr/viz-bin/VizieR?-source = II/246. The Gaia and Spitzer IRAC data are obtained from https://gea.esac.esa.int/archive/ and https://irsa.ipac.caltech.edu/cgi-bin/Gator/nph-scan?submit=Select&projshort=SPITZER, respectively. We used the following links https://archive.stsci.edu/hlsp/eleanor and https://adina.feinste.in/eleanor/ to obtain TESS data.

REFERENCES

Andre P., Ward-Thompson D., Barsony M., 1993, ApJ, 406, 122
Appenzeller I., Mundt R., 1989, A&AR, 1, 291A
Attridge J. M., Herbst W., 1992, ApJ, 398, 61
Bailer-Jones C. A. L., Rybizki J., Fouesneau M., Demleitner M., Andrae R., 2021, AJ, 161, 147
Balona L. A., et al., 2011, MNRAS, 413, 2403
Barrado y Navascués D., Zapatero Osorio M. R., Béjar V. J. S., Rebolo R., Martín E. L., Mundt R., Bailer-Jones C. A. L., 2001, A&A, 377, L9
Bessell M. S., Brett J. M., 1988, PASP, 100, 1134
Bica E., Bonatto C., Dutra C. M., 2008, A&A, 489, 1129
Bouvier J., Cabrit S., Fernández M., Martín E. L., Matthews J. M., 1993, A&AS, 101, 485
Bouvier J. et al., 2007, A&A, 463, 1017
Broeg C. et al., 2006, A&A, 450, 1135
Cantat-Gaudin T., Anders F., 2020, A&A, 633, A99
Canto Martins B. L., Gomes R. L., Messias Y. S., 2020, ApJS, 250, 20
Cieza L., Baliber N., 2007, ApJ, 671, 605
Cohen J. G., Persson S. E., Elias J. H., Frogel J. A., 1981, ApJ, 249, 481
Cohen R. E., Sarajedini A., 2012, MNRAS, 419, 342
Cutri R. M. et al., 2003, yCAT, 2246
Edwards S. et al., 1993, AJ, 106, 372
Erickson R. R., 1971, Astron. Astrophys., 10, 270
Feinstein A. D., Montet B. T., Foreman-Mackey D., 2019, PASP, 131, i4502
Gaia Collaboration, 2016, A&A, 595, A1
Gaia Collaboration, 2021, A&A, 649, A1
Ghosh P., Lamb F. K., 1979, ApJ, 234, 296
Girardi L., Bertelli G., Bressan A., Chiosi C., Groenewegen M. A. T., Marigo P., Salasnich B., Weiss A., 2002, A&A, 391, 195
Godoy-Rivera D., Pinsonneault M. H., Rebull L. M., 2021, ApJS, 257, 46
Gondoin P., 2018, A&A, 616, 154
Guetter H. H., 1992, Astron. J., 103, 197
Gutermuth R. A. et al., 2008, ApJ, 674, 336

Herbst W., Herbst D. K., Grossman E. J., Weinstein D., 1994, AJ, 108, 1906
Herbst W., Bailer-Jones C. A. L., Mundt R., 2001, ApJ, 554, 197
Herbst W., Bailer-Jones C. A. L., Mundt R., Meisenheimer K., Wackermann R., 2002, A&A, 396, 513
Hojaev A. S., Chen W. P., Lee H. T., 2003, Astron. Astrophys. Trans., 22, 799
Herbst W. et al., 2004, IAUS, 202, 341
Huang P. C. et al., 2019, ApJ, 871, 183
James D. J. et al., 2010, A&A, 515, 100
Johnstone D. et al., 2018, ApJ, 854, 31
Joy A. H., 1945, ApJ, 102, 168
Kearns K. E., Herbst W., 1998, AJ, 116, 261
Koenigl A., 1991, ApJ, 370, L39
Knote M. F., Caballero-Nieves S. M., Gokhale V., Johnston K. B., Perlman E. S., 2022, ApJS, 262, 10
Lada C. J., 1987, Proc. IAU Symp 115, Star Forming Regions. D. Reidel Publishing Co., Dordrecht, p. 1
Lamm M. H., Bailer-Jones C. A. L., Mundt R., Herbst W., Scholz A., 2004, A&A, 417, 557
Lomb N. R., 1976, Astrophys. Space Sci., 39, 447
Martín E. L., Brandner W., Bouvier J, Luhman K. L., Stauffer J., Basri G., Zapatero Osorio M. R., Barrado y Navascués D., 2000, ApJ, 543, 299
Massey P., Johnson K. E., Degioia-Eastwood K., 1995, ApJ, 454, 151
Meibom S., Mathieu R. D., Stassun K. G., Liebesny P., Saar S. H., 2011, ApJ, 733, 115
Meibom S., Mathieu Robert D., Stassun K. G., 2009, ApJ, 695, 679
Meyer M. R., Calvet N., Hillenbrand L. A., 1997, AJ, 114, 288
Morales E. F. E., Wyrowski F., Schuller F., Menten K. M. 2013, A&A, 560, A76
Morales-Calderón M. et al., 2011, ApJ, 733, 50
Morales-Calderon M. et al., 2012, ApJ, 753, 149
Nordhagen S., Herbst W., Rhode K. L., Williams E. C., 2006, AJ, 132, 1555
O'Connell D. J. K., 1951, Publ. Riverview Coll. Obs., 2, 85
Ostriker E. C., Shu F. H., 1995, ApJ, 447, 813
Pandey J. C., Karmakar S., Joshi A., Sharma S., Bhushan P. S., Pandey A. K., 2019, RAA, 19, 7
Pigulski A., Kolaczkowski Z., Kopacki G., 2000, AcA, 50, 113
Rangwal G., Yadav R. K. S., Durgapal A. K., Bisht D., 2017, PASA, 34, 68
Riaz B., Martín E. L., Tata R., Monin J. -L., Phan-Bao N., Bouy H., 2012, MNRAS, 419, 1887
Ricker G. R. et al., 2015, J. Astron. Tel. Instr. Syst., 1, 014003
Sagar R., Joshi U. C., 1981, Astrophys. Space Sci., 75, 465
Scargle J. D., 1982, ApJ, 263, 835
Shi H. M., Hu J. Y., 1999, Astron. Astrophys. Suppl. Ser., 136, 313
Shu F., Najita J., Ostriker E., Wilkin F., Ruden S., Lizano S., 1994, ApJ, 429, 781
Siess L., Dufour E., Forestini M., 2000, A&A, 358, 593
Stetson P. B., 1987, PASP, 99, 191
Stetson P. B., 1992, J. R. Astron. Soc. Can., 86, 71
Stone D. G., 1988, Astron. J., 96, 1389
Torres G., 2010, AJ, 140, 1158
Turner D. G., 1979, JRASC, 73, 74
Zahajkiewicz E., 2012, AN, 333, 1086

This paper has been typeset from a TEX/LATEX file prepared by the author.